Land Conservation and the Clean Energy Transition: Evidence from U.S. Wind and Solar Development*

Meredith Fowlie* Charles A. Taylor†

*UC Berkeley and NBER †Harvard University and NBER

March 2026

Preliminary and Incomplete

Abstract

We study the interactions between land conservation policy and renewable energy development using two decades of U.S. wind and solar grid interconnection applications linked to fine-grained geospatial data. A model of competitive site selection shows that the welfare implications of land use protections depend critically on the correlation between conservation value and private development potential. When this correlation is weak, targeted restrictions can steer projects away from ecologically sensitive areas without meaningfully raising technology deployment costs. Estimating a sequential model of site entry and project advancement, we find that wetlands protections and conservation easements significantly deter development. Correlations between engineering profitability and measures of conservation value are near zero, implying that the landscape is amenable to well-targeted conservation policy. However, our estimates of the 'soft costs' imposed by the existing patchwork of restrictions appear substantial. Ongoing counterfactual analysis aims to quantify these compliance burdens and assess how alternative land use regimes could reshape the spatial allocation of renewable energy development.

*We appreciate feedback from participants in seminars at UCLA, Yale, University of Texas, Cornell University, University of Toronto, NC State/Duke, University of Chicago (Coase), Electric Power Research Institute (EPRI), International Alpine Workshop on Energy Economics and Policy (Switzerland), ETH Zurich, Harvard Kennedy School, Toulouse School of Economics, CEE-M Montpellier, University of Hawaii, UC Berkeley Energy Camp, Lawrence Berkeley National Laboratory, and the ASSA 2025 meeting.

1 Introduction

The current decarbonization strategy in the United States, as in most countries, emphasizes a zero-carbon power system and economy-wide electrification. Implementing this strategy will require an unprecedented and accelerated expansion of wind and solar electricity generation infrastructure (Williams et al. 2021; Larson 2020). Wind and solar energy are far more land-intensive than fossil or nuclear alternatives (Davis et al. 2023). Tens of millions of acres could be required to support new clean energy infrastructure over the next 30 years, constituting roughly 0.5% to 7.7% of the continental United States.[1]

Many Americans will benefit from a large-scale clean energy deployment which can deliver economy-wide greenhouse gas emissions reductions and local air quality improvements (Fell et al. 2021). But the relatively large spatial footprint of wind and solar electricity generation can introduce conservation tradeoffs because biodiversity loss is largely driven by land-use change (Newbold et al. 2015; Jaureguiberry et al. 2022). Tens of millions of acres of ecologically sensitive land could be negatively impacted by clean energy resource development.

This paper investigates the interactions between land conservation and the clean energy transition. We address three related questions: How fundamental is the conflict between conservation priorities and renewable energy development? Are existing land use protections limiting infrastructure deployment? And if so, are these restrictions significantly increasing the costs of clean energy expansion?

We begin with a conceptual framework to elucidate the conditions under which land use protections can improve the efficiency of renewable energy siting. In our model, competitive developers evaluate potential sites that vary in terms of electricity generation potential, private development costs, and conservation value. The welfare implications of land use protections depend critically on the correlation between these attributes: when conservation value and economic potential are weakly correlated well-targeted restrictions can steer development away from ecologically sensitive sites without systematically sacrificing the most productive energy projects. When the correlation is strong, restrictions force developers off their most lucrative sites, raising the cost of the energy transition. The welfare implications of existing land use protections are therefore an empirical question.

We bring nearly two decades of wind and solar project proposals to bear on this question,

[1] The wide range primarily reflects the large indirect footprint of wind due to turbine spacing requirements. The direct land footprint of wind is comparatively small. The land area of the continental US is about 2 billion acres (8 million km^2). Under the baseline E+ projection (Larson 2020), onshore wind and solar directly impact 39,000 km^2 (0.5% of land), but their overall footprint (including spacing) is 589,000 km^2 (7.4% of land).

pairing project-level interconnection queue data with information on approximately 60,000 potential sites drawn from NREL's national renewable energy supply curves. For each site — potential and proposed — we construct time-varying measures of electricity generation potential, techno-economic costs, land use restrictions, and local community demographics.

Taken together, these data reveal some new empirical facts that are germane to renewable energy resource development. First, using vintage-specific engineering simulations, we are documenting how renewable energy supply curves have shifted over time as falling technology costs and improving capacity factors have been partially offset by rising curtailment rates (not yet included in this working draft – coming soon!). Second, we construct annual snapshots of the high-voltage transmission network from 1985 to 2023 that can be used to document how the distance to transmission (a key determinant of project costs) has fallen as networks have expanded. Finally, using fine-grained measures of three conservation policies—wetlands protections under the Clean Water Act, habitat protections under the Endangered Species Act, and conservation easements under Section 170(h) of the Internal Revenue Code — we find that correlations between measures of conservation value and standard engineering measures of profitability are near zero, ranging from 0.03 to 0.06 for both wind and solar sites. This finding is good news for land conservation policy, as it suggests that well-targeted land use protections need not come at significant cost to the clean energy transition.

Building on this conceptual foundation, we estimate a sequential model of renewable energy project siting that tracks developers through two observed decision points: the choice to enter an interconnection queue, and the subsequent decision to proceed with a project or withdraw. In the first stage, we model queue entry as the purchase of an option — developers incur sunk application costs based on expected site-level surplus, retaining the right to withdraw if conditions deteriorate. In the second stage, we model the decision to proceed, correcting for the fact that queue entrants are a selected sample using a control function approach. Identification of the cost wedges imposed by land use restrictions comes from within-market, within-cohort variation in the stringency of land use restrictions, conditional on detailed site-level techno-economic attributes. A key feature of our approach is that we calibrate these controls using the same engineering models and data sources that are made available to developers to inform renewable energy site prospecting. This helps ensure that residual variation in land use restrictions is not proxying for differences in underlying site quality or economic attractiveness. The remaining identification argument is that the forces governing where wetlands, critical habitat, and conservation easements fall — hydrology, biology, and landowner tax incentives — operate largely independently of the economic forces governing where renewable energy development is profitable.

This modeling exercise reveals three main findings. First, the key attributes emphasized by standard capacity expansion modeling — technology investment costs, electricity generation potential, and distance from transmission infrastructure — are significant determinants of entry decisions, confirming that developers respond to economic fundamentals in predictable ways. Second, existing land use protections impose meaningful costs on project development: wetlands protections and conservation easements significantly reduce the probability of proposing and completing renewable energy projects in affected areas. Third, we find that some site attributes enter decisions differently at the initial prospecting stage versus the subsequent project commitment stage, consistent with developers gathering more precise information as the process unfolds and weeding out the least viable sites early on. This suggests that an analysis focused exclusively on queue entrants would underestimate the deterrent effect of wetlands protections, for example, since these regulations are already shaping which sites developers consider worth pursuing in the first place.

With model estimates in hand, we are well-positioned to evaluate the likely implications of alternative land use restriction regimes for renewable energy siting — an analysis that is in progress. Our first pass takes the level of renewable energy investment as given, consistent with binding state-level procurement targets, and asks how profit-maximizing developers would reallocate investments across sites under alternative land use restrictions. Preliminary results focusing on wind projects exclusively suggest that land use restrictions have a meaningful effect on the spatial allocation of development. Removing wetlands regulations and/or easements reshuffles a significant share of projects across sites. Whereas impacts on techno-engineering costs are moderate, the implied compliance and permitting cost savings are substantial. These counterfactual simulations are a work in progress.

Our work contributes to a growing empirical literature in economics of renewable energy development. One line of inquiry has investigated the impacts of government incentives — including tax credits, subsidies, and feed-in tariffs — on wind and solar deployment (Borenstein 2012; Aldy et al. 2023; Deschenes et al. 2023). A parallel literature has documented some of the formidable complications that developers face in bringing projects to completion, including regulatory and permitting risk, community opposition, fragmented property rights, and the growing burden of interconnection queue backlogs (Jarvis 2021; Rand and Hoen 2017; Susskind et al. 2022; Winikoff and Parker 2024; Johnston et al. 2023; Kashner 2026). What is missing from this empirical literature is a systematic examination of how land conservation policies shape project siting and development costs — the question at the center of our paper. Importantly, ex ante capacity expansion models have begun to incorporate conservation concerns into long-run renewable deployment planning (Wu et al. 2023;

Shawhan et al. 2020), but these models are not designed to recover how developers actually respond to those constraints in practice. Our data-driven, revealed preference approach begins to fill this gap.

We also contribute to the literature on land conservation policy. A recent review identifies the effect of protected area policy on economic activity as a key open question (Reynaert et al. 2024), and several recent papers have begun to make progress — examining the efficacy and distributional impacts of conservation instruments including protected areas, the Endangered Species Act, and conservation easements (Grupp et al. 2023; Frank et al. 2025; Harstad 2023). Taylor and Druckenmiller 2022 and Druckenmiller et al. 2026 provide direct estimates of the land market effects of Clean Water Act jurisdiction that we draw on in calibrating our counterfactual simulations. Aronoff and Rafey 2026 study the effects of wetland conservation incentives on private development decisions in Florida. Building on their conceptual framework, we focus on a different margin — the siting of renewable energy infrastructure at national scale.

Finally, our findings speak to ongoing policy debates about the tension between conservation and infrastructure development. Concerns that land use protections impose excessive costs on development have animated a broader permitting reform debate (Klein and Thompson 2025), including bills recently passed by the U.S. House targeting both NEPA environmental review and Clean Water Act jurisdiction. In the renewable energy context, policymakers are developing tools to steer development toward low-conflict sites — from California's Desert Renewable Energy Conservation Plan to the Bureau of Land Management's Western Solar Plan. Our results speak directly to the feasibility and design of such approaches. The weak correlation between conservation value and economic potential suggests that steering is achievable, but the substantial compliance and hassle costs of navigating the existing patchwork of restrictions point to clearer ex ante zoning as a more efficient path forward.

The remainder of the paper is organized as follows. Section 2 presents the conceptual framework. Section 3 describes the data and empirical context. Section 4 details the empirical framework and identification strategies. Section 5 presents estimation results. Section 6 describes the counterfactual analysis. Section 7 concludes.

2 Conceptual Framework

We introduce a stylized model of renewable energy project siting in which competitive, price-taking project developers evaluate a large set of potential sites. Developers form expectations

about site-specific revenues and costs and make decentralized entry decisions based on a latent net surplus index. The spatial allocation of renewable energy development is therefore governed by a distribution of site-level profitability. This framework provides a tractable link between observable site characteristics and the probability of project entry which we exploit in the empirical analysis.

Renewable energy project site selection

A large set of potential sites in a regional electricity market, indexed by $i \in \mathcal{I}$, vary along several observable dimensions. Whereas capacity expansion models focus predominantly on electricity generation potential q_i and techno-economic costs (e.g. technology investment costs, interconnection costs) c_i, we extend our model to consider land conservation value v_i, land use restrictions l_i, and local community demographics d_i. We make a distinction between private capital and resource costs c_i, the costs of complying with land use restrictions l_i, and the costs of negotiating with local communities. We define a compliance cost function $\gamma(l)$ to capture the permitting, redesign, and mitigation costs that developers can incur when land use restrictions constrain the siting process. We define a negotiation cost function $\eta(d)$ to capture any costs incurred to secure community acceptance.

We characterize electricity generation potential, costs, and conservation impacts in terms of net present values (NPV) evaluated at entry time $t = 0$ over a project time horizon T using a discount factor $\delta \in (0, 1)$:

$$q_i \equiv \sum_{t=0}^{T} \delta^t q_{it}, \qquad c_i \equiv C_i^{\text{CAPEX}} + \sum_{t=0}^{T} \delta^t \, c_{it}^{\text{OPEX}}, \qquad v_i \equiv \sum_{t=0}^{T} \delta^t v_{it}.$$

For now, we assume that the conservation value function is additively separable in v_i. This abstracts away from spatial spillovers that can make the conservation value of preserving one location partly a function of the conservation status of nearby parcels. We further assume that site attributes are jointly distributed across space $(q_i, c_i, v_i, l_i) \sim f(q, c, v, l)$.[2]

Developers act as price takers in electricity, land, and capital markets. Agents form expectations about the profitability of a site based on information available at the time of entry. We define a latent net surplus index:

$$\pi_i \;\equiv\; P q_i \;-\; c_i \;-\; \gamma(l_i) \;-\; \eta(d_i) \;+\; \omega_i,$$

[2] We assume finite means $\mu_q = \mathbb{E}[q_i]$, $\mu_c = \mathbb{E}[c_i]$, $\mu_v = \mathbb{E}[v_i]$, $\mu_l = \mathbb{E}[l_i]$; variances $\sigma_q^2, \sigma_c^2, \sigma_v^2, \sigma_l^2$; and correlations $\rho_{qc}, \rho_{qv}, \rho_{cv}, \rho_{lv}, \rho_{lc}, \rho_{lq}$.

where P is the prevailing contract price at the time of entry, $\omega_i \sim F_\omega$ captures unobserved, site-specific cost components, and the remaining terms correspond to the revenue and cost primitives defined above. Site i will be pursued if $\pi_i \geq 0$, i.e., if expected revenues cover all private costs including compliance and negotiation burdens. With this formulation, we will not recover cross-site substitution elasticities in the discrete choice sense. Instead, we aim to recover how site characteristics shift the distribution of latent surplus and thus the probability of entry.

The equilibrium spatial allocation of selected sites is governed by a net-surplus-based selection rule. If we assume that all sites that appear ex ante profitable get developed, the total quantity of renewable energy supplied is:

$$S(P) \;=\; \int q_i \cdot \mathbf{1}\{\pi_i \geq 0\}\, dF(i).$$

Aggregating across sites yields an implicit supply relationship in which generation increases with the contract price as more marginal sites become profitable (all else held constant). Market demand for renewable electricity generation is $Q^d(P)$. The equilibrium price P^* is pinned down by a market-clearing condition:

$$S(P^*) \;=\; Q^d(P^*).$$

This equilibrium condition determines the marginal project. Land use restrictions and community opposition enter as site-specific cost wedges that shift the distribution of latent net surplus, thereby altering both the level and composition of site development. In settings with binding procurement targets, this framework admits an equivalent representation in which sites are selected in order of decreasing expected surplus until the target is met. We leverage this interpretation in our counterfactual analysis.

Costs and benefits of land use restrictions

Land use restrictions take a variety of forms (e.g., wetlands protections, habitat protections, and conservation easements). When the stringency or scope of land use restrictions changes from l to l', developers face a modified distribution of net surplus, which in turn can alter both the set of projects that are privately viable and the equilibrium price of renewable energy contracts. Let y_i denote whether site i is developed under policy regime l:

$$y_i(l) = \mathbb{1}\{\pi_i(l) \geq 0\},$$

where $\pi_i(l) \equiv P^*(l)q_i - c_i - \gamma(l_i) - \eta(d_i) - \omega_i$ and $P^*(l)$ is the equilibrium price induced by the distribution of latent net surplus under l.[3]

Total social welfare under regime l is given by:

$$W(l) \;=\; \int_0^{S(P^*(l))} P^d(x)\,dx \;-\; \sum_i y_i(l)\,(c_i + \gamma(l_i) + \eta(d_i) + v_i). \tag{1}$$

This formulation corresponds to a competitive benchmark in which decentralized developers internalize private development, compliance, and negotiation costs, but do not internalize conservation damages. Equation eq:Welfare does not explicitly account for the pollution impacts associated with a change in renewable energy investment. To the extent that land use restrictions primarily reallocate renewable energy investments across sites within a regional market, these emissions impacts will not be large. Future work will explore the potential for emissions impacts.

Privately optimal siting decisions may be inefficient from a social perspective in the presence of conservation externalities. In principle, land use restrictions can improve welfare by discouraging development on sites with high conservation value v_i, but they also increase the cost of supplying renewable energy by excluding low-cost sites or increasing compliance costs at marginal projects. The net welfare impact depends on how restrictions reshape the composition of developed sites and, in equilibrium, the marginal cost of supply. The welfare impact of moving from l to l' is:

$$\Delta W = \int_{S(P^*(l))}^{S(P^*(l'))} P^d(x)\,dx - \sum_i \left(y_i(l') - y_i(l)\right)(c_i + \gamma(l_i') + v_i). \tag{2}$$

Equation 2 provides a direct link to our empirical analysis. We estimate how observable site characteristics shift the probability of development and use these estimates of cost primitives to recover changes in site selection probabilities under counterfactual land use restrictions, $y_i(l') - y_i(l)$. Because monetary valuations of conservation damages v_i are not directly observed, we will instead report implied trade-offs between development costs and non-

[3] Changes in land use restrictions that raise costs only for inframarginal projects leave the marginal unit unchanged and therefore do not affect the equilibrium price, operating instead through higher costs for already-selected sites. By contrast, restrictions that bind at or near the margin can shift the equilibrium price $P^*(l)$.

monetary measures of land conservation, such as the cost per acre of land protected.

Economic potential, conservation value, and welfare gains

To characterize the economic costs imposed by land use restrictions, it will be useful to define a baseline surplus measure in the absence of land use restrictions or other permitting frictions:

$$\pi_i^{TE} \equiv Pq_i - c_i,$$

which we refer to as *techno-economic surplus*. In the absence of land use restrictions and other permitting frictions, developers select sites with $\pi_i^{TE} + \omega_i \geq P$. Land use restrictions introduce additional site-specific costs that potentially alter the set of developed sites. The welfare impacts of land use restrictions will depend on the correlations between techno-economic surplus and conservation values across sites. Intuitively, restricting development at a given site avoids conservation damages v_i but may require replacing that site with a lower π_i^{TE}.

Proposition 1. *The welfare gains from land use restrictions are decreasing in the correlation between conservation value v_i and techno-economic surplus π_i^{TE}.*

Intuition. The welfare impact of a restriction is the ecological benefit (avoided v_i) net of the **economic opportunity cost** (forgone π_i^{TE}). The sign and magnitude of this net gain are driven by the correlation $\rho_{v\pi}$. Varying the correlation $\rho_{v\pi}$ helps build intuition for this proposition [4]:

- **Case 1: Negative Correlation** If $\rho_{v\pi} < 0$, high conservation value implies low profitability. The most ecologically sensitive sites are unattractive to developers. Because market forces already steer developers away from high-v sites, land use restrictions are largely redundant.

[4] To motivate this proposition more formally, consider a policy that targets sites where $v_i > \bar{v}$. The expected economic cost per restricted site is $\mathbb{E}[\pi_i^{TE} \mid v_i > \bar{v}]$. Under the assumption of joint normality (or a linear projection), this is:

$$\mathbb{E}[\pi_i^{TE} \mid v_i > \bar{v}] = \mu_\pi + \rho_{v\pi} \left(\frac{\sigma_\pi}{\sigma_v} \right) (\mathbb{E}[v_i \mid v_i > \bar{v}] - \mu_v) \tag{3}$$

The expected forgone surplus is strictly increasing in $\rho_{v\pi}$. As $\rho_{v\pi} \to 1$, the policy targets the most lucrative projects, maximizing opportunity costs. As $\rho_{v\pi} \to -1$, the probability that a restricted site was in the privately viable set $\mathcal{A}_l(P)$ approaches zero. Net welfare is therefore a concave function of $\rho_{v\pi}$, with the highest gains realized when the correlation is low enough to preserve development on high-margin sites but high enough to ensure the policy prevents actual ecological damage. See Appendix A.2 for the full derivation.

- **Case 2: Positive Correlation** If $\rho_{v\pi} > 0$, high conservation value sites are also highly profitable. Areas with the most sensitive habitats are also the most lucrative sites for energy production. Targeted land use restrictions will increase the costs of renewable resource development.
- **Case 3: Weak Correlation ($\rho_{v\pi} \approx 0$).** Unlike Case 1, some sites with high conservation value are also highly profitable. Unlike Case 2, high conservation value sites are not systematically the highest-yield locations. Land use restrictions can discourage development on sites with high conservation value without systematically targeting the highest-value energy projects.

This proposition characterizes the conditions under which land use restrictions *could* improve welfare, but it does not by itself determine whether those conditions are met in practice. Whether existing land use protections are actually impacting renewable energy siting choices is an empirical question. In what follows, we examine correlations between measures of techno-economic profits and measures of conservation value to assess the potential for welfare-improving land protections. Finding close-to-zero correlations in these empirical comparisons, we turn to investigate how existing land protections have been impacting renewable energy resource siting and associated costs.

3 Data and Descriptive Evidence

Our analysis pairs nearly two decades of wind and solar projects entering U.S. interconnection queues with a large set of potential development sites drawn from NREL supply curve grid-cells. For each location—both proposed and potential —we collect detailed information along the five dimensions described above: electricity generation potential, techno-economic costs, land use restrictions, conservation value, and local community demographics. We begin by describing the interconnection queue process and the structure of our dataset. We then highlight the novel aspects of our data construction. Finally, we present descriptive evidence on the relationship between economic potential, conservation value, and site selection—directly testing the conditions underlying Proposition 1. Detailed variable construction methodology is provided in the Data Appendix.

3.1 Data overview and project lifecycle

The process of developing a renewable energy project proceeds through several stages. Developers first screen potential locations using available data on resource quality, costs, and land availability. After securing site control, they submit an interconnection request to the relevant transmission operator, entering a queue that initiates engineering studies of grid reliability impacts and required network upgrades (Rand et al. 2024). Over 70% of projects that enter the queue are ultimately withdrawn; among those that persist, developers execute a formal interconnection agreement (IA) with the transmission provider. Figure 1a summarizes annual queue entry trends and Figure 1b maps the geographic distribution of projects; Figure 1c shows that interconnection success rates have been declining since 2015, particularly for wind, and Figure 1d confirms that projects reaching IA are strong predictors of eventual commercial operation.

Our dataset includes both proposed and potential sites. First, project-level interconnection queue data compiled by LBNL track all wind and solar projects entering U.S. queues since 2005, aggregating records from the seven organized wholesale electricity markets and 35 additional utilities, covering more than 85% of U.S. electricity load. We geocode these records to obtain spatially precise project locations, enabling us to locate siting decisions in both time and space—a first for the complete U.S. interconnection queue (see Data Appendix for methodology). Second, we draw on NREL's national renewable energy supply curve datasets, which identify approximately 60,000 technically viable development sites across the continental United States based on standardized engineering and land-use screening criteria. We use these supply curve gridcells to construct potential project sites representing locations where developers could have proposed projects but did not. Each site is assigned a queue entry year and project capacity by sampling from the distribution of the nearest actual developer, preserving temporal and capacity patterns within each market. The resulting analysis sample pairs several thousand queue entrants with roughly ten times as many possible sites for each technology, beginning in 2005 for wind and 2010 for solar. Exact sample sizes are reported in the summary statistics tables.

3.2 Novel data contributions

Our analysis requires assembling site-level measures of economic potential, land use restrictions, and conservation value at a resolution finer than any prior study of renewable energy siting. Three aspects of our data construction are particularly novel: (i) vintage-specific calibration of engineering profits using project-level simulations, (ii) national-coverage mea-

surement of three major conservation policies at the project-footprint scale, and (iii) construction of a credible choice set from NREL supply curve data (described above). We briefly summarize each dimension here; detailed construction methodology is in the Data Appendix.

3.2.1 Techno-economic site attributes

We simulate annual electricity generation potential for each site using NREL's PySAM software with vintage-year-specific technology parameters, adjusted for projected degradation and ISO-specific curtailment. Because turbine technology has evolved significantly over our sample period (e.g., taller towers and larger rotors for wind; increasing inverter loading ratios for solar), the generation potential of different locations has changed differently over time. Expected revenues combine ISO-year-technology-specific Power Purchase Agreement (PPA) prices with federal tax incentives (ITC and PTC) and accelerated depreciation benefits, computed at multiple queue-entry offsets to reflect conditions at the time of operation rather than entry.

Development costs include time-varying distance to the nearest high-voltage transmission line ($\geq$69 kV), measured using annual snapshots of the transmission network from 1985 to 2023 (Preonas, Sweeney, and Taylor 2026). The time-varying nature of this measure is important: substantial grid expansion over our sample period means that sites considered remote in 2005 may be well-connected by 2020, and most prior studies use a static snapshot that misses this variation.

We also measure local land acquisition costs from CoreLogic property transaction data; property tax liabilities that account for state-level variation in the tax treatment of renewable energy projects (Uebelhor et al. 2021; Kashner 2026); and year-specific capital expenditure estimates from LBNL and NREL's Annual Technology Baseline. We control for terrain roughness and land cover composition. See the Data Appendix for construction details. The fine resolution of our data captures within-market site selection that coarser analyses would miss.

Wind queue projects exhibit capacity factors 5 percentage points above the NREL potential site (28% vs. 23%), and 77% of this gap is within-ISO microsite selection rather than cross-market sorting (Figure 14). For solar, the capacity factor gap is negligible, consistent with solar siting driven by grid access rather than irradiance (Figure 3). Significant within-market variation extends beyond resource quality to transmission distance, land costs, and conservation exposure—variables for which site-level measurement is essential and county- or state-level aggregation would risk ecological fallacy.

3.2.2 Land use restrictions l_{it}

Wetlands. Geospatial data on water features come from the US Fish and Wildlife Service's National Wetlands Inventory (NWI). Section 404 of the Clean Water Act protects wetlands by requiring costly permits for activities that disturb wetlands and streams, effectively raising development costs (Taylor and Druckenmiller 2022; Druckenmiller et al. 2026). We also use predictions from a machine learning algorithm that estimates property-level probabilities of wetland regulation across the US (Greenhill et al. 2024).

Critical habitat and avian sensitivity. US Fish and Wildlife Service (FWS) shapefiles on locations of critical habitat for threatened and endangered species approximate the risk of a project to potential violations under the Endangered Species Act (Ferris and Frank 2021; Auffhammer et al. 2020). The boundary data include both polygons and lines (which largely denote rivers or streams). For the latter, we include a 300m buffer. For each project site, we count the number of overlapping FWS critical habitat designations, with separate counts for all listed species, endangered species only, and bird species.

We also measure exposure to avian habitat using the National Audubon Society's Important Bird Areas (IBA) database, which identifies sites of critical importance for bird conservation across the United States (Wells et al. 2005). The IBA program has designated over 2,700 sites covering approximately 417 million acres, encompassing key breeding, wintering, and migratory stopover habitats. For each project location, we count the number of overlapping IBA polygons and apply the inverse hyperbolic sine transformation. Wind-wildlife conflicts—particularly bird and bat mortality from turbine collisions—are a prominent source of regulatory risk and public opposition for wind energy projects, making avian habitat a potentially important determinant of both siting decisions and project outcomes. Accordingly, we use avian habitat as the primary habitat measure in the wind specifications and endangered species critical habitat in the solar specifications.

Conservation easements. Conservation easements are legally binding agreements in which landowners permanently surrender development rights to a conservation organization in exchange for tax benefits under Section 170(h) of the Internal Revenue Code. Conservation easements now cover more than 38 million acres of US land, nearly twice the footprint of the USDA's Conservation Reserve Program. They enjoy bipartisan support and have grown faster than more traditional federal conservation efforts. The annual deductions associated with conservation easements cost the government $2.3 billion per year in foregone tax revenues, with additional state-level incentives and impacts on local property tax collections. This cost is on par with the budgets of major federal conservation and land management enti-

ties like the Bureau of Land Management ($1.7 billion budget), US Fish and Wildlife Service ($1.9 billion), and the National Park Service ($3.5 billion).[5] IRS tax return data show that the average conservation easement donor receives a $1.2 million annual tax deduction—far more than any other type of charitable donation (Table 8).

In general, conservation easements prohibit new infrastructure development. Wind and solar projects cannot legally be placed on land under conservation easement—such commercial activities are generally forbidden under the terms of the easement contract. Even if a project is sited on unencumbered land, an easement located on a nearby property in the way of necessary transmission infrastructure can jeopardize project success. A map of easements across the continental US is shown in Figure 10a.

We compile conservation easement boundaries from three sources: the National Conservation Easement Database (NCED), The Nature Conservancy (TNC) land trust records, and the NRCS easement database. We drop federal and state-owned conservation lands and focus on private easements. For each project site, we compute the total acreage under conservation easement within a range of buffer radii from 100m to 6000m. Our primary specification uses the 3000m (3km) buffer, which we find captures the distance at which nearby easements most strongly affect development outcomes—consistent with easements impeding access routes and transmission infrastructure rather than only direct site overlap. We apply the inverse hyperbolic sine (IHS) transformation to address the heavy right skew of easement acreage.

Where easement establishment dates are available, we decompose the total into pre-entry acres (established before the project's queue entry year) and post-entry acres (established within five years after entry). This temporal decomposition is important for identification: pre-existing easements represent a constraint that developers observe when selecting sites, while post-entry easements may reflect strategic conservation responses to proposed development.[6]

Government-owned protected land. Data from USGS GAP PAD-US v2.0 provide a parcel-based inventory of government fee-owned protected areas. Such areas are excluded from potential development, and we drop any placebo project points that fall within 1000m of such lands.

[5] The Inflation Reduction Act included $1.4 billion in additional funding for conservation easements beyond the Farm Bill allocation of $450 million per year for USDA's Agricultural Conservation Easements Program.

[6] Easement date information is incomplete: approximately 28% of NCED records lack an establishment year, with the share exceeding 90% in Texas and 75% in North Carolina (Figure 15b). The TNC and NRCS records have complete date coverage. In addition, reporting lags mean that recent years likely undercount new easements.

Local ordinances and preemption. Data on local zoning restrictions come from NREL's comprehensive databases of local ordinances for siting wind and solar energy projects (Lopez et al. 2023). These county-level data record the year in which each jurisdiction adopted ordinances regulating renewable energy development—including setback requirements, noise limits, height restrictions, and outright moratoria. We construct a pre-entry indicator equal to one if the ordinance was enacted more than two years before the project's queue entry, and a post-entry indicator for ordinances in effect during the queue process. Separately, we code state-level siting preemption laws that override local zoning authority for energy projects. Several states have enacted such laws in recent years, including New York, California, Illinois, Michigan, Maryland, and Minnesota, effectively limiting the ability of local governments to block renewable energy development through zoning restrictions. These siting preemption laws are distinct from the state-level property tax treatment categories described above.

3.2.3 Demographics d_{it}

We measure local demographic characteristics using gridded income and population data from the U.S. Census Bureau's Privacy-Protected Gridded Environmental Impacts Frame (Voorheis et al. 2024). The Gridded EIF provides population counts and household income deciles on a fixed 0.01-degree grid (approximately 1.2 km^2) across the continental United States. For each project site, we assign income deciles and population density from the nearest gridcell, averaged over the 2000–2020 period. These variables proxy for local economic conditions and potential community opposition—higher-income and more densely populated areas may face stronger resistance to nearby energy development.

3.2.4 Conservation value measures v_{it}

We use several measures of conservation value that do not enter the regression models directly but are used to assess the correlation between conservation value and economic potential (Proposition 1) and to evaluate conservation impacts in the counterfactual analysis. Technology-specific measures of conservation value come from 250m raster maps created by The Nature Conservancy as part of their Power of Place initiative (Jones et al. 2023). The environmental impact scoring system quantifies the ecological impact separately for solar and wind development, assigning scores to various categories of land based on their environmental importance (e.g., wetlands score the highest due to their ecological value). We also use a measure of "protection-weighted range-size rarity" computed using habitat suitability models for 2,216 taxonomically-diverse species (Hamilton et al. 2022).

3.3 Descriptive evidence

We now examine the empirical relationship between economic potential, conservation value, and observed site selection—the conditions underlying Proposition 1.

Weak correlation between economic potential and conservation value. Table 1 reports pairwise correlations between our calibrated measure of engineering profitability and several measures of conservation value across the pooled sample of potential and actual development sites. Across all metrics—TNC environmental impact scores, wetland extent, critical habitat, and bird habitat—correlations with engineering profits are near zero, ranging from -0.03 to 0.06 for both wind and solar sites. These weak correlations satisfy the conditions of Proposition 1 under which land use restrictions can improve welfare at low economic cost: high-conservation-value sites are not systematically the most profitable development opportunities, so well-targeted restrictions need not sacrifice the highest-value energy projects. The right columns of Table 1 show that existing land protections are at least partially well-targeted: wetlands regulation is strongly correlated with actual wetland extent (0.53), though easements show weaker correlations with conservation metrics—a pattern we revisit in the estimation results.

Selection on land use restrictions. Tables 2 and 3 reveal systematic differences in conservation exposure across potential entrants, queue entrants, and projects that sign interconnection agreements. Wind entrants have lower wetland share than potential sites (0.02 vs. 0.05), fewer nearby easements (65 acres within 3km vs. 110), and lower TNC conservation scores (4.77 vs. 6.40). For projects that successfully reach interconnection, easement exposure falls further to 43 acres within 3km. A similar pattern holds for solar on easements at close range. These raw comparisons are suggestive but cannot distinguish regulatory deterrence from correlated site attributes. For example, flat agricultural land that is cheaply acquired for development may also tend to have fewer wetlands and less easement encumbrance. The econometric model addresses this by conditioning on a rich set of site-level economic attributes within market-year cohorts.

4 Empirical strategy

The conceptual framework introduced in Section 2 characterizes site selection through a net surplus threshold: site i is developed if and only if $\pi_i \geq 0$. Land use restrictions and the potential for local opposition enter as cost wedges $\gamma(l_i)$ and $\eta(d_i)$ that reduce net surplus and thereby lower the probability of development. We now take this framework to data,

estimating the parameters of the latent surplus function empirically.

Specifying the empirical analog of our conceptual site selection model is complicated by the fact that renewable energy development is, in reality, considerably messier than the one-shot entry decision we consider in Section 2. Developers entering an interconnection queue must navigate a sequence of engineering studies, cost assessments, and permitting milestones that can span a decade or more. We observe two decision points in this process: the choice to enter an interconnection queue, and the subsequent decision to proceed to an interconnection agreement or withdraw. We exploit this sequential structure by estimating a two-stage model. In the first stage, we model queue entry as the purchase of an option — developers commit sunk costs based on expected surplus, retaining the right to withdraw if conditions deteriorate. In the second stage, we model the decision to proceed, correcting for the fact that queue entrants are a selected sample. This structure allows site attributes to enter decisions differently at the initial prospecting stage versus the subsequent commitment stage — a feature of the data we document in the results.

4.1 Stage 1: Queue Entry

In the first stage, denoted $t = 0$, project developers observe site traits ($q_{i,0}$, $c_{i,0}$, $l_{i,0}$, $d_{i,0}$) and market-level state variables (prevailing, technology-specific electricity contract prices P_0, market-level policy shocks, etc.). For expositional ease we abstract away from the choice of solar versus wind technology; we account for technology-specific attributes in the empirical estimation.

Developers can apply to develop site i in market m and year y after incurring a sunk application cost $K_{i,0}$. We define an initial net surplus index evaluated on time-of-entry expectations:

$$\pi_{i,m,y,0} \equiv \underbrace{\bar{P}_{m,y,0}\, q_{i,y,0}}_{\text{expected revenue}} - \underbrace{c_{i,y,0}}_{\text{project costs}} - \underbrace{\gamma(l_{i,y,0})}_{\text{compliance costs}} - \underbrace{\eta(d_{i,y,0})}_{\text{negotiation costs}} + \underbrace{\xi_{m,0}}_{\text{market-cohort effect}} + \underbrace{\delta_{y,0}}_{\text{year effect}}, \tag{4}$$

where $\xi_{m,0}$ captures market-cohort-average surplus (including conditions that developers observe but the researcher does not) and δ_y similarly captures year-of-sample effects. Attributes are calibrated to reflect costs and market conditions at the year of entry y. For ease of exposition, we hereafter drop the y subscript and the δ_y fixed effects that are included in our empirical specifications.

Because developers face long wait times in interconnection queues, they anticipate that conditions at the time of construction will likely differ from those at entry. We capture this

with a site-specific stochastic shock ω_i to project value that is not yet realized at the time of entry—for example, unexpected interconnection upgrade costs, newly discovered land use restrictions, or changes in local opposition. A project can be withdrawn if the realized net surplus turns negative. Thus, developers evaluate the *option* to proceed by taking an expectation over ω_i:

$$G(\pi_{i,m,0}) \;=\; \mathbb{E}_{\omega}[\max\{0,\; \pi_{i,m,0} + \omega_i\}]\,,$$

where $G(\cdot)$ is strictly increasing in $\pi_{i,m,0}$. Under A1 below, the distribution of ω_i is common within a market-year cohort.By taking the expectation at entry, ω_i will be integrated out into the option value function $G(\cdot)$. Market-cohort fixed effects absorb the parameters $G(\cdot)$, leaving only the site-specific variation in $\pi_{i,m,0}$ to drive differences in entry probability across sites.

The developer's total latent value of entry is:

$$V_{i,0} \;=\; -K_{i,0} + G(\pi_{i,m,0}) + \varepsilon_{i,0},$$

where $\varepsilon_{i,0}$ captures site-specific private information that the developer observes at the time of entry but that is unobservable to the researcher—for example, early-stage site assessments, landowner relationships, or local permitting intelligence. Unlike ω_i, which represents anticipated *future* uncertainty, $\varepsilon_{i,0}$ is part of the developer's *current* information set; it is $\varepsilon_{i,0}$ that rationalizes probabilistic entry among observationally similar sites. The application decision rule is:

$$\text{apply } (a_{i,0} = 1) \iff V_{i,0} \geq 0.$$

Static representation of the dynamic queue application choice: Under the following conditions, the dynamic queue application problem is observationally equivalent to a static binary-choice model with market-cohort and year fixed effects:

A1: Cohort-common option value. Within a market×year cohort c, expected contract prices, application costs $K_{i,0}$, and the option value function $G(\cdot)$ are common across sites. This requires not only that market-level conditions $\bar{P}_{m,0}$ and $K_{i,0}$ are cohort-common, but also that the distribution of ω_i does not vary systematically across sites within a market- cohort. Under A1, $\xi_{m,0}$, $K_{i,0}$, and $G(\cdot)$ are all absorbed by the market-cohort fixed effect $\xi_{c,0}$.

A2: Within-cohort selection on observables. Conditional on observed site covariates $X_{i,0}$ (which include measures of $q_{i,0}$, $c_{i,0}$, $l_{i,0}$, $d_{i,0}$, and other land controls), the site-level private information $\varepsilon_{i,0}$ is mean-independent of $l_{i,0}$ and $d_{i,0}$ within cohort. This is

the key identification assumption: conditional on techno-economic site attributes, land use restrictions and local demographics are uncorrelated with the developer's private information about the site.

A3: Common withdrawal frictions. Expected withdrawal costs are cohort-common (hence absorbed by α_c) or negligible.

A4: Idiosyncratic profitability shock. $\varepsilon_{i,0}$ is additive and i.i.d. across sites with a standard logistic or normal distribution, generating a logit or probit link function.

Proposition 2. *Under A1–A4, a local linearization of $\gamma(l_{i,0})$, $\eta(d_{i,0})$, and $c_{i,0}$ yields:*

$$\Pr(a_{i,0} = 1 \mid X_{i,0},\, l_{i,0}, d_{i,0},\, \alpha_c) \;=\; \Lambda(\alpha_c + X'_{i,0}\beta - l'_{i,0}\gamma - d'_{i,0}\eta), \qquad \gamma > 0,$$

where α_c absorbs $\xi_{m,0}$, $K_{i,0}$, and the option value $G(\cdot)$; $X_{i,0}$ captures site-specific measures of $c_{i,0}$ and $\bar{P}_{m,0}q_{i,0}$.

Sketch. By A1, $K_{i,0} = K_c$ and $G(\cdot) = G_c(\cdot)$ within cohort. The entry condition $V_{i,0} \geq 0$ is therefore equivalent to $\varepsilon_{i,0} \geq K_c - G_c(\pi_{i,m,0})$. Because $G_c(\cdot)$ is strictly increasing, there exists a cohort-specific threshold κ_c such that this condition reduces to $\pi_{i,m,0} \geq \kappa_c$. Substituting the linearized components of $\pi_{i,m,0}$ and setting $\alpha_c \equiv -\kappa_c$ (which absorbs $\xi_{m,0}$, K_c, and the constant terms of the cost functions) yields:

$$\alpha_c + X'_{i,0}\beta - \gamma\, l_{i,0} + \varepsilon_{i,0} \geq 0.$$

Under A4, $\varepsilon_{i,0}$ has a standard logistic distribution and the probability of entry takes the form $\Lambda(\alpha_c + X'_{i,0}\beta - \gamma\, l_{i,0})$. Note that ω_i does not appear: it has been integrated out into $G_c(\cdot)$ and absorbed by α_c. □

Identification: Estimating the parameters of the latent surplus function requires two distinct identification arguments. The first concerns the techno-economic controls $X_{i,0}$. To recover the structural cost and revenue parameters, our measures must credibly proxy for the information developers act on when screening sites. This is plausible because we calibrate our measures of these variables (e.g. contract prices, electricity generation potential, technology component costs, distance from transmission infrastructure) using the same tools and data sources that are made available to private developers (e.g. market and technology specific PPA prices, vintage-specific PySAM simulations of generation potential, ATB capital cost benchmarks, and time-varying transmission distance). One potential complication is that land prices and associated property tax estimates could partly reflect *anticipated* renew-

able energy development in an area, introducing endogeneity. We address this by controlling for pre-sample land transaction prices and verify robustness to dropping land prices from the specification entirely.

The second identification argument requires that, conditional on $X_{i,0}, \xi_{m,o}, \delta_0$, residual variation in land use restrictions is uncorrelated with developers' private information $\varepsilon_{i,0}$. Several considerations support plausibility. As shown in Table 1, land use restrictions are approximately uncorrelated with standard ex ante profitability across the full sample of potential sites, suggesting that the forces governing where restrictions fall operate largely independently of the economic forces governing where development is profitable. The spatial distribution of wetlands and critical habitat is governed by hydrological and biological criteria administered by federal agencies. Conservation easements reflect landowner tax incentives and land trust priorities. Neither process responds directly to renewable energy potential or capital costs. That said, our terrain and land cover controls may not fully absorb all spurious correlations. Future work will explore instrumentation strategies (e.g. changes in the generosity of federal and state tax incentives for easement creation). We interpret current estimates as conditional correlations that are informative about the sign and order of magnitude of cost wedges, and we present robustness checks using alternative control sets.

4.2 Stage 2: Interconnection Agreement

The first stage recovers how site attributes shape the initial decision to enter the queue. But entry is only the first hurdle: the majority of projects that enter the queue ultimately withdraw before signing an interconnection agreement. The second stage exploits this variation, asking what distinguishes projects that advance from those that do not. This stage is conceptually distinct from the first — developers are now making a commitment decision with updated information about site-specific costs and market conditions that was unavailable at entry. Recovering how land use restrictions shape this commitment decision requires accounting for the fact that queue entrants are not a random draw from the population of potential sites; projects that survived the first stage are systematically different from those that did not. We address this with a control function approach, using the first-stage model to correct for non-random selection into the queue.

Whereas queue entry dates are precisely recorded, the timing of subsequent withdrawal decisions and interconnection agreements are not so carefully tracked throughout our time period. We do have excellent records, post 2020, of final project status. This allows us to identify which projects have ultimately withdrawn and which projects remain active.

We define a 'second stage' outcome using this available information, limiting the sample to projects that enter the queue prior to 2022 to allow time to observe withdrawal decisions. We define a second stage indicator $a_{i,1}$ that equals 1 if the project is still advancing and/or active; $a_{i,1} = 0$ if the project has formally withdrawn. Relative to the entry stage, this second stage decision is made with updated information about project-specific costs (e.g., interconnection upgrade requirements) and market conditions. We calibrate all variables to reflect one information available three years following queue entry (we assess the robustness of our results to alternative time lags).

We define a Stage 2 net surplus index evaluated at post-entry expectations, denoted $t = 1$:

$$\pi_{i,1} \equiv \underbrace{\bar{P}_1\, q_{i,1}}_{\text{expected revenue}} - \underbrace{c_{i,1}}_{\text{project costs}} - \underbrace{\gamma(l_{i,1})}_{\text{compliance costs}} - \underbrace{\eta(d_{i,1})}_{\text{negotiation costs}} - \underbrace{\xi_{i,1}}_{\text{unobserved costs}}. \quad (5)$$

This index has the same general structure as $\pi_{i,0}$ in Stage 1. One key difference is that $\pi_{i,1}$ is observed only for queue entrants. We drop projects that entered after 2022 because these projects have not had much time to collect the information that would lead them to withdraw (the average time between entry and project withdrawal is 3-4 years).

Because selection into Stage 2 depends on $\pi_{i,0}$, the distribution of $\xi_{i,1}$ among entrants need not match the population distribution, and naive estimation of the second-stage decision on the selected sample would yield biased estimates. We address this with a control function approach. Because market conditions shift substantially between queue entry and IA signing: PPA prices, capital costs, and technology parameters at $t = 0$ influence which projects enter the queue but enter $\pi_{i,1}$ only through their updated $t = 1$ values. This time variation means that the Stage 1 index $\pi_{i,0}$ contains information about selection that is not fully captured by the Stage 2 covariates $X_{i,1}$, providing the variation needed to construct a valid control function. Specifically, under a standard single-index selection structure, $\mathbb{E}[\xi_{i,1} \mid S_i = 1, \cdot] = h(\pi_{i,0})$ for some unknown function $h(\cdot)$. We approximate $h(\cdot)$ using the generalized residual from the Stage 1 logit:

$$\widehat{CF}_i = \frac{a_i - \hat{p}_i}{\hat{p}_i(1 - \hat{p}_i)},$$

where a_i is the Stage 1 entry indicator and $\hat{p}_i$ is the predicted entry probability. This yields the estimating equation:

$$\Pr(y_i = 1 \mid S_i = 1) = \Lambda\Big(\alpha_{c,1} + X'_{i,1}\theta - l'_{i,1}\gamma - d'_{i,1}\eta + \delta\, \widehat{CF}_i\Big), \quad (6)$$

where $\alpha_{c,1}$ is a market×year cohort fixed effect, $X_{i,1}$ captures site-specific measures of $c_{i,1}$ and $\bar{P}_1 q_{i,1}$, and δ is the coefficient on the control function. A statistically significant $\hat{\delta}$ indicates the presence of selection bias that would have distorted naive estimates of model parameters.

As in Stage 1, developers retain an option to cancel after signing the IA.[7] Let $H(\pi_{i,1}) \equiv \mathbb{E}_\omega[\max\{0, \pi_{i,1} + \omega_i\}]$ denote the Stage 2 option value, defined analogously to $G(\pi_{i,0})$ in Stage 1; $H(\cdot)$ is strictly increasing under standard shocks. The developer's total latent value of signing is:

$$V_{i,1} \;=\; -K_{i1} + H(\pi_{i,1}) + \varepsilon_{i,1},$$

where K_{i1} is the sunk cost of proceeding and $\varepsilon_{i,1}$ is a site-specific shock known to the developer but latent to the researcher, defined analogously to $\varepsilon_{i,0}$ in Stage 1. The decision rule is:

$$\text{sign } (y_i = 1) \iff V_{i,1} \geq 0.$$

Static representation of the interconnection decision. We rationalize a static representation of the IA decision by invoking A1–A4 at $t = 1$ (with all cohort-common primitives, selection on observables, withdrawal frictions, and the idiosyncratic shock re-defined at Stage 2) and adding one condition that addresses the sequential structure:

A5: Time-varying covariates. Market conditions — including PPA prices and capital costs — vary between queue entry ($t = 0$) and the IA decision ($t = 1$). Their $t = 0$ values shift selection into Stage 2 but enter $\pi_{i,1}$ only through updated $t = 1$ values, ensuring that $\pi_{i,0}$ provides variation in $\widehat{CFCF}_i$ that is not collinear with $X_{i,1}$.

Proposition 3. *Under A1–A5, a local linearization of $\gamma(l_{i,1})$, $\eta(d_{i,1})$, and $c_{i,1}$ yields the estimating equation in (6), where including $\widehat{CFCF}_i$ removes the selection bias arising from non-random entry into Stage 2.*

Sketch. By A1 at $t = 1$, $K_{i1} = K_{c1}$ within cohort. Monotonicity of $H(\cdot)$ then implies $V_{i,1} \geq 0 \Leftrightarrow \pi_{i,1} \geq \kappa_{c,1}$ for a cohort-specific threshold $\kappa_{c,1}$. Setting $\alpha_{c,1} \equiv -\kappa_{c,1}$ and applying the same linearization as in Proposition 2 yields the single-index form in (6). The conditional mean of $\xi_{i,1}$ among entrants equals $h(\pi_{i,0})$; substituting $\widehat{CFCF}_i$ and including it with coefficient δ removes the resulting bias. Under A5, the time variation in covariates ensures $\widehat{CFCF}_i$ is not collinear with $X_{i,1}$. □

[7] In practice, IAs may involve deposits or liquidated damages. We treat the cohort-common component of these frictions as absorbed by the fixed effect; site-specific penalties can be added to $X_{i,1}$.

5 Estimation Results

First stage: queue entry

We estimate the queue entry model using a logit specification with market × period fixed effects. The dependent variable equals one if a project is proposed at a given location and zero otherwise. Tables 4 and 6 report average marginal effects for wind and solar respectively; Figures 4a and 5a summarize these graphically. All covariates are standardized, so coefficients represent the effect of a one-standard-deviation change. Unless otherwise noted, we report coefficients from the preferred specification that includes all conservation and demographic controls. To put these estimates into perspective, the baseline entry rate across the set of gridded NREL potential sites is approximately 10% for wind sites and 22% for solar sites.

The key economic determinants for wind projects (Table 4) enter with expected signs and are precisely estimated. A one-standard-deviation increase in annual output per MW raises the probability of queue entry by 5.1 percentage points, consistent with developers selecting sites with superior wind resources. Distance to the nearest high-voltage transmission line is the single largest deterrent to entry: a one-standard-deviation increase reduces entry probability by 8.7 percentage points, reflecting the substantial interconnection costs associated with remote siting. The share of developed land is positively associated with entry (+4.7 percentage points), likely capturing proximity to existing infrastructure and demand.

For solar projects (Table 6), the most economically significant predictor of entry is distance to transmission, with a marginal effect of −15.7 percentage points per standard deviation. This is roughly three times the magnitude of the corresponding solar resource coefficient (+5.2 percentage points), consistent with the descriptive evidence in Figure 3 showing that solar capacity factors vary little across potential sites, so that grid access rather than resource quality is the binding constraint on site selection. The share of developed land enters positively and is the second-largest predictor (+8.4 percentage points). Elevation variation significantly deters solar entry (−1.9 percentage points), with a larger magnitude than for wind (−1.5 percentage points), consistent with the importance of flat terrain for utility-scale photovoltaic installations. Population and income are also significant negative predictors of solar entry, suggesting that solar developers avoid densely settled or high-cost areas (which may proxy for the likelihood of local opposition).

Turning to the conservation variables that are the focus of this paper, two results stand out. First, conservation easements in the immediate project vicinity (within 100 meters) significantly deter queue entry for both wind and solar. The marginal effect is −1.1 percentage

points for wind and −0.6 percentage points for solar, implying that a one-standard-deviation increase in local easement coverage reduces entry probability by approximately 11% and 3% relative to the respective baseline rates. Second, the share of the surrounding area classified as wetland reduces entry probability by 1.4 percentage points for wind and 1.1 percentage points for solar. The wind wetlands effect is significant across specifications; the solar effect is smaller and reaches significance only in the most saturated specification.

Bird habitat is a significant negative predictor of solar entry in specifications that include conservation controls (−0.6 percentage points, $p < 0.05$), though the effect is attenuated in the most saturated specification. The remaining conservation variables—endangered species critical habitat, local ordinances, and state preemption laws—are small and not statistically significant for either technology. Land price enters negatively but loses significance once property tax controls are included, consistent with land costs being a small share of total project costs.

Second stage: interconnection and project success

We next estimate the interconnection model, in which the dependent variable equals one if a queued project advances to an interconnection agreement or gets built rather than withdrawing (or otherwise failing). Tables 5 and 7 report average marginal effects; Figures 4b and 5b display the results graphically. The baseline success rate is 25% for wind and 34% for solar, conditional on queue entry.

For wind projects (Table 5), the economic predictors shift in relative importance between stages. Net capital expenditure emerges as the dominant predictor of interconnection success, with a one-standard-deviation increase reducing interconnection probability by 18 percentage points. Annual revenues enter positively (+8 percentage points), as expected. Distance to transmission, which was the strongest deterrent at the entry stage, is no longer a significant predictor of interconnection conditional on entry—consistent with developers already having screened out remote sites, leaving insufficient residual variation to exploit at this stage.

For solar (Table 7), annual revenues are a significant positive predictor (+2.2 percentage points). The net capital expenditure coefficient is positive and significant in specifications with year fixed effects (+3.1 to +3.9 percentage points), but small and insignificant when ISO-period fixed effects absorb cohort-level cost trends (+0.9 percentage points). This unexpected sign likely reflects the fact that solar capital costs fell substantially and heterogeneously over our sample period; within market-year cohorts, residual variation in estimated capital expenditure may not capture meaningful project-level cost differences after condition-

ing on the fixed effects that absorb common technology trends. We note that the revenue coefficient, which is less subject to this concern, enters with the expected sign and is significant in most specifications. Land value (-1.2 percentage points) and developed share (-1.8 percentage points) are both significant negative predictors of solar interconnection, and elevation variation also enters negatively (-2.0 percentage points).

The central finding at the interconnection stage is that conservation easements in the project vicinity (within 3km of geolocation centroid) have a robust negative effect on project advancement for both technologies. For wind, the marginal effect is -2.0 percentage points per standard deviation; for solar it is -1.9 percentage points. Given baseline interconnection rates of 25% and 34%, these represent reductions of approximately 8% and 6% in the probability of project completion. These effects are stable across specifications and survive the inclusion of the selection correction term.

In contrast to the entry stage, wetland share does not enter significantly at the interconnection stage for either technology. This asymmetry suggests that wetlands protections operate primarily by deterring initial site selection rather than causing projects to fail once they are in the queue. Developers appear to screen out wetland-exposed sites early in the prospecting process, so that conditional on having entered the queue, residual wetland exposure does not predict withdrawal. An analysis focused exclusively on queue entrants would therefore underestimate the full deterrent effect of wetlands protections by missing their influence on the pre-entry screening stage.

The selection correction term is statistically insignificant in both the wind and solar interconnection models. This suggests that non-random selection into the queue does not introduce substantial bias into the interconnection-stage estimates, though it does not rule out selection on unobservables that the control function fails to capture.

Bird habitat, endangered species critical habitat, and local ordinances are not significant predictors of interconnection for either technology.

A consistent pattern across both stages and technologies is that spatially precise restrictions—conservation easements—are significant deterrents, while broader range-level designations such as critical habitat for birds or endangered species are less so. This distinction is intuitive. Easements are recorded on specific parcels with clearly delineated boundaries; they directly constrain land assembly, site layout, access roads, and transmission corridor routing on a spatial scale commensurate with project footprints. Critical habitat designations, by contrast, cover large geographic ranges that may encompass thousands of potential sites. A project sited within a designated range can often avoid the specific features that triggered

the designation, and the regulatory consequences of habitat overlap are uncertain ex ante and negotiated through project-specific consultation. The result is that range-level designations generate diffuse rather than site-specific cost signals, which may not be sufficiently concentrated to alter developer behavior at the margins we observe.

From Estimates to Cost Impacts

The estimated coefficients from our logit models are identified only up to scale, and so cannot be directly interpreted as dollar-denominated cost wedges. To aid interpretation, we report average marginal effects of a one-standard-deviation change in each covariate on the probability of queue entry and interconnection. These marginal effects are the primary objects of interest in our estimation results.

To assess the economic magnitudes implied by land use restrictions, we exploit the fact that capital expenditure—a variable measured in dollars— enters the latent surplus index. Under the assumption that the logit scale parameter is constant within a market-year cohort, the ratio of two coefficients recovers the corresponding ratio of latent surplus primitives. Specifically, the ratio of the land use restriction coefficient to the capital expenditure coefficient, $\hat{\gamma}/\hat{\beta}_K$, provides a money-metric estimate of the implicit cost wedge per unit of the restriction, expressed in units of capital expenditure. We use this ratio to translate marginal effects into approximate dollar-equivalent impacts, with the caveat that this normalization requires the scale parameter to be stable across sites and cohorts—an assumption we assess in robustness checks.

We report these dollar-equivalent estimates alongside the marginal effects as a secondary summary of economic magnitudes, but emphasize that the marginal effects themselves are the primary, assumption-minimal objects of inference.

Placeholder for results to come

This section has summarized the empirical results we have generated thus far. We are refining and expanding this modeling exercise in a variety of ways. This includes accommodating random parameters to allow for heterogeneity in how developers perceive capital costs, transmission distances, contract prices, among other factors. Using a random parameter logit specification, we will estimate the distribution of implied monetary measures of key components using the ratio of site attribute coefficients and the capital cost coefficient.

6 Counterfactual Analysis

Our empirical results establish that existing land use restrictions—particularly wetlands and conservation easements—meaningfully deter both site selection and project completion. We now turn to explore the welfare implications of these restrictions, using the estimated two-stage model to simulate how renewable energy siting and associated costs would vary under counterfactual land use regimes. The welfare equation derived in Section 2 (Equation 1) provides the organizing framework.

Approach

We simulate project siting under counterfactual land use restrictions while holding RPS-driven total generation (GWh) fixed within each market-cohort. By 2011, a majority of U.S. states had adopted Renewable Portfolio Standards establishing renewable energy generation targets. Treating these targets as binding and exogenous, we can simulate project siting over the period 2012–2021 under observed market conditions and counterfactual scenarios that remove specific land use restrictions, holding market-level capacity investment fixed.

The simulation proceeds in three steps. First, we calibrate baseline surplus indices at observed prices and land use restrictions for all sites. We rank sites in descending order and select projects until the observed GWh target for each market-cohort is met. Second, we recalibrate land use restriction measures to reflect a counterfactual regime and adjusting land prices accordingly, following the land market response estimates of druckenmiller2026. Third, we re-rank all sites using the counterfactual siting index and again select projects until the same GWh target is met. Because the simulations do not require monetizing conservation value directly, we summarize conservation impacts in terms of the physical attributes—wetland acreage, habitat acres—of sites that shift in and out of the development portfolio across scenarios.

Preliminary findings

The counterfactual simulations are ongoing, and we reserve a full presentation of results for a subsequent draft. Nevertheless, the preliminary findings are broadly consistent with the conceptual framework and descriptive evidence presented above, and we summarize the main patterns here.

The scenarios we have considered thus far (e.g. removing easements, removing wetlands

protections) causes a meaningful share of projects to relocate to different sites, while aggregate electricity generation remains approximately unchanged by construction. The reshuffled projects tend to have modestly higher engineering costs, reflecting that wetlands protections have been steering development toward sites that happen to be somewhat more capital-intensive. Notably, the reduction in "hassle" costs captured by our monetized $l_i'\gamma$ estimates are more significant. Removing wetlands regulation is associated with a reduction in transmission distance for the counterfactual portfolio, consistent with wetlands tending to cluster in low-lying areas near existing transmission corridors. As expected, the acres of wetlands impacted by development increase under the counterfactual, confirming that wetlands regulation is doing ecological work—steering projects away from sensitive sites rather than simply adding frictions to an otherwise undistorted allocation.

Taken together, these (highly preliminary) results suggest that the impacts of changes in land use restrictions on *techno-economic costs* incurred to deliver a given level of renewable electricity generation could be moderate in aggregate terms, though the spatial reallocation of development would be substantial. This is consistent with the near-zero correlation between conservation value and engineering profitability documented in Section 3: because the landscape does not systematically concentrate high-conservation-value land at the most profitable development sites, restricting such land primarily changes where projects are built rather than how much it costs to build them. However, the 'soft-costs' associated with negotiating existing restrictions are economically significant, such that changes in regulator regimes can appreciably impact total deployment costs.

Results thus far are partial equilibrium: they account for land market responses but hold electricity contract prices fixed. Additional counterfactual scenarios—including the removal of conservation easements, combined removal of all restrictions, and endogenous PPA price adjustment—are in progress.

7 Conclusion

This paper investigates three related questions about the interaction between land conservation and clean energy deployment.

First, *how fundamental is the conflict between land conservation priorities and renewable energy development?* We develop a conceptual framework showing that the welfare implications of land use protections depend critically on the correlation between conservation value and private economic potential. Empirically, we find that this correlation is weak: measures

of conservation value are approximately uncorrelated with engineering profitability for both wind and solar sites. This means that well-targeted land use restrictions can steer projects away from ecologically sensitive areas without systematically targeting the most profitable development opportunities.

Second, *are land use restrictions limiting clean energy infrastructure development?* Using two decades of wind and solar interconnection data, we estimate a sequential model of queue entry and interconnection decisions. We find that existing land protections—wetlands regulations under the Clean Water Act and conservation easements under Section 170(h)—significantly reduce the probability of both proposing and completing renewable energy projects in affected areas. Conservation easements have a robust negative effect on interconnection probability that is concentrated at distances below 3 km.

Third, *have land use restrictions significantly increased deployment costs?* Our preliminary counterfactual analysis suggests that removing wetlands regulation would reshuffle a substantial share of projects across sites but would have modest effects on aggregate generation costs. This is consistent with the weak correlation result: because conservation value is approximately orthogonal to private cost efficiency, land protections primarily change *where* projects are built rather than *how much* it costs to build them.

Relatedly, Aronoff and Rafey 2026 show that wetland offset markets generated large private gains from trade but shifted conservation away from flood-vulnerable areas. This underscores that the spatial reallocation of development we document can have environmental consequences beyond the ecological dimensions we measure.

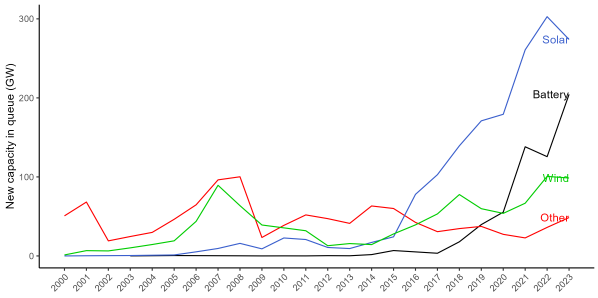
These findings have implications for policymakers navigating the tension between rapid clean energy deployment and land conservation. The results suggest that the current portfolio of land use protections is not imposing large costs on the clean energy transition, and that well-targeted restrictions can preserve ecologically valuable areas at relatively low economic cost. At the same time, the analysis highlights the importance of ensuring that conservation easements and other protections are well-targeted to high-conservation-value lands, rather than serving primarily as vehicles for tax benefits.

Several limitations warrant mention. Our geolocation of queue projects introduces measurement error that could attenuate estimated effects. The completeness of conservation easement data varies across states and time periods. And the counterfactual analysis assumes that RPS targets are binding and exogenous—assumptions that may not hold in all markets. Ongoing work extends the counterfactual simulation to include endogenous PPA price responses and conservation easement removal scenarios, accommodates richer hetero-

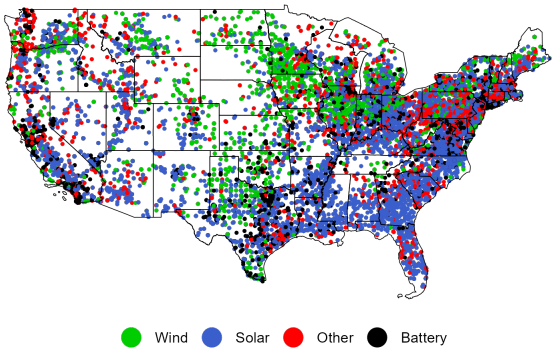
geneity in the choice model, investigates how changes in the scope of wetland protections under the Clean Water Act have affected siting over our sample period, and uses satellite imagery to estimate realized land use impacts following infrastructure development.

Figures and Tables

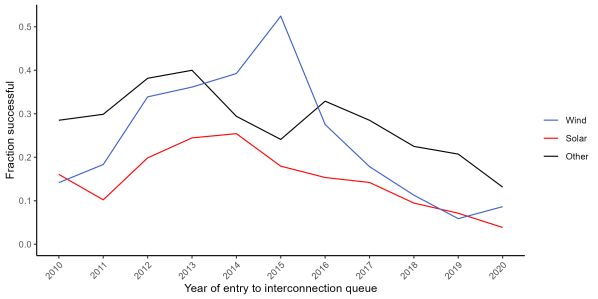
Figure 1: Interconnection Queue: Entry Trends, Project Locations, and Outcomes



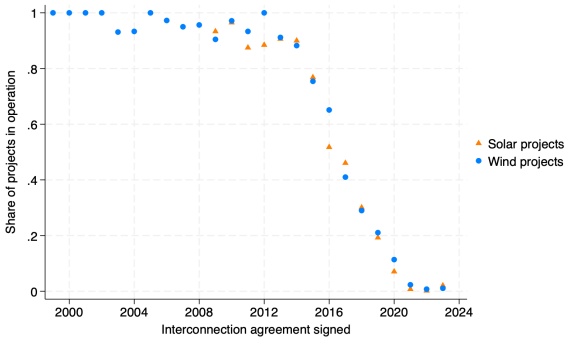
(a) Annual queue entry by technology (GW)



(b) Location of queue projects, 2000–2023



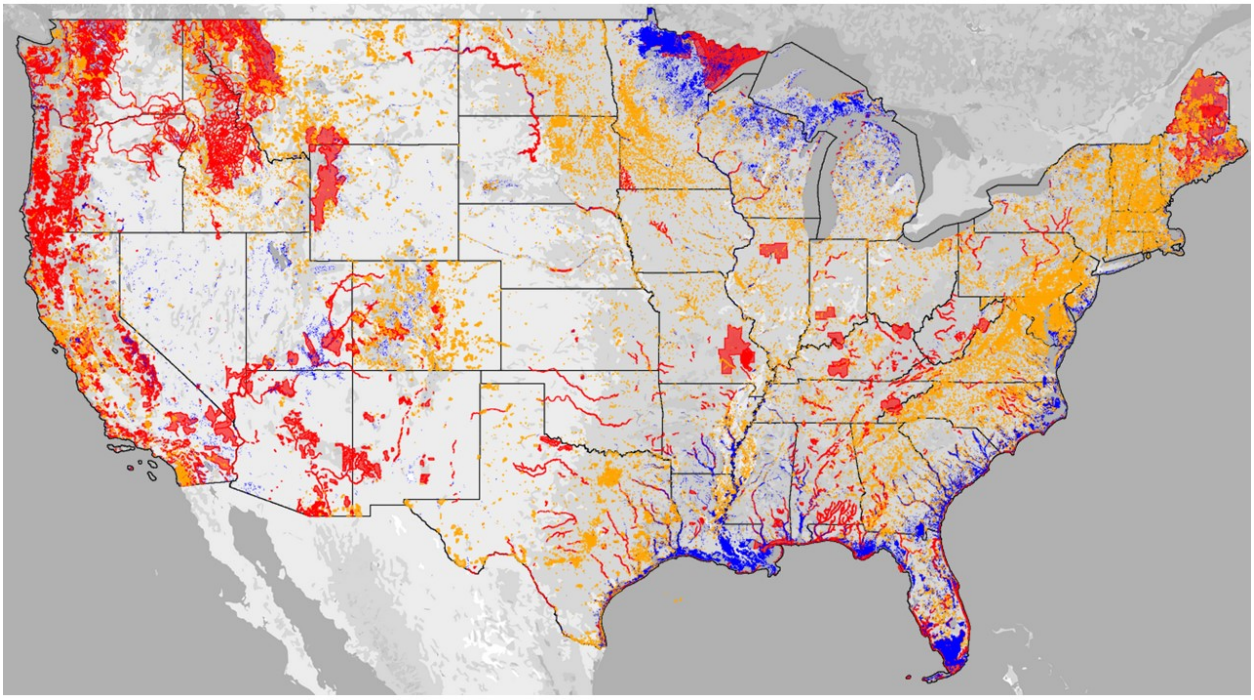
(c) Share receiving interconnection agreement



(d) Share reaching commercial operation

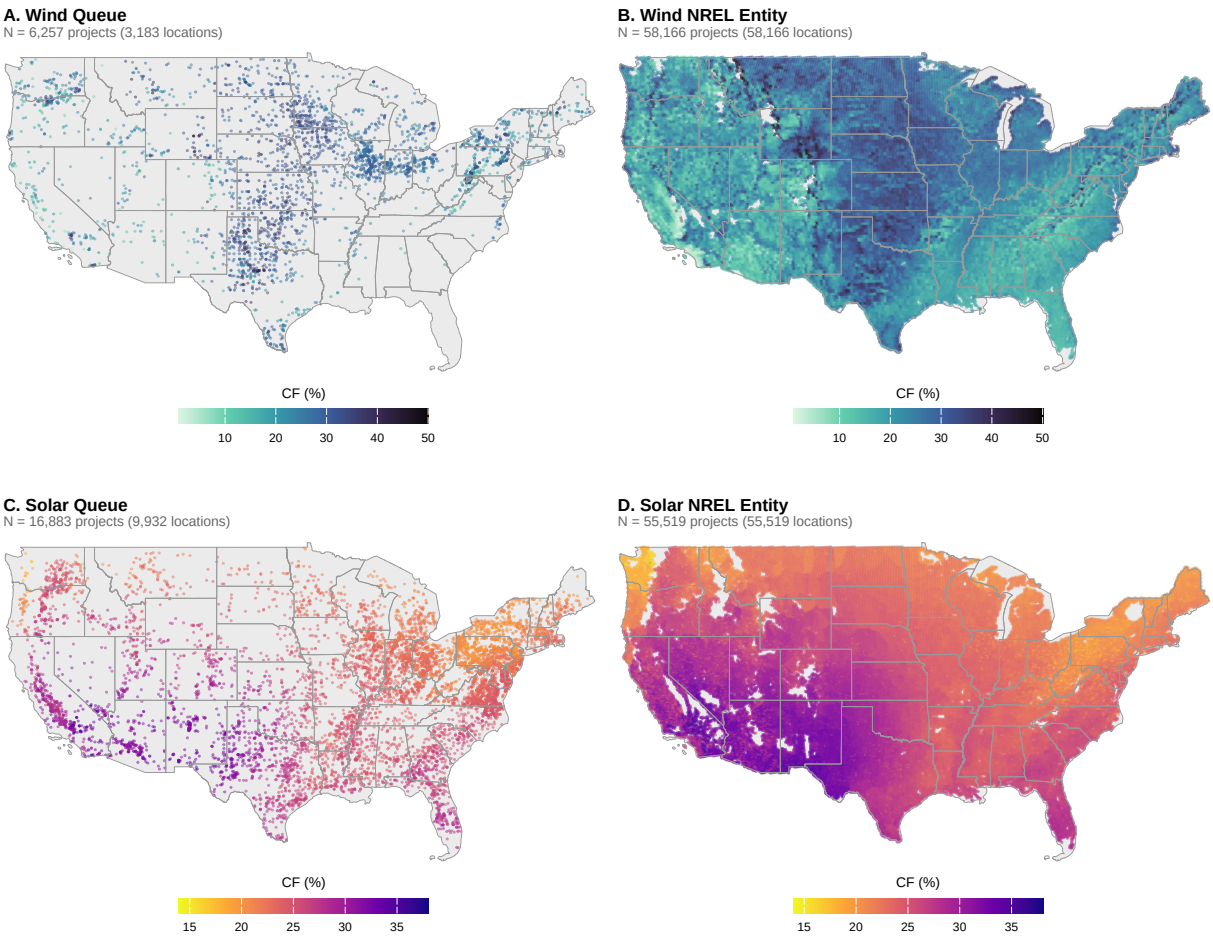
Notes: Panel (a) summarizes annual queue entry by technology in terms of planned capacity (GW). Panel (b) maps all projects by technology type. Panel (c) shows the share of entrants that ultimately receive an interconnection agreement (2021–2023 excluded to allow sufficient time). Panel (d) shows the share of IA-signing projects that reach commercial operation. Data from Lawrence Berkeley National Lab.

Figure 2: Spatial Distribution of Land Use Restrictions



Notes: Map shows the spatial distribution of three types of land use restrictions considered in this analysis: wetlands regulated under Section 404 of the Clean Water Act, critical habitat designated under the Endangered Species Act, and conservation easements recorded in the National Conservation Easement Database.

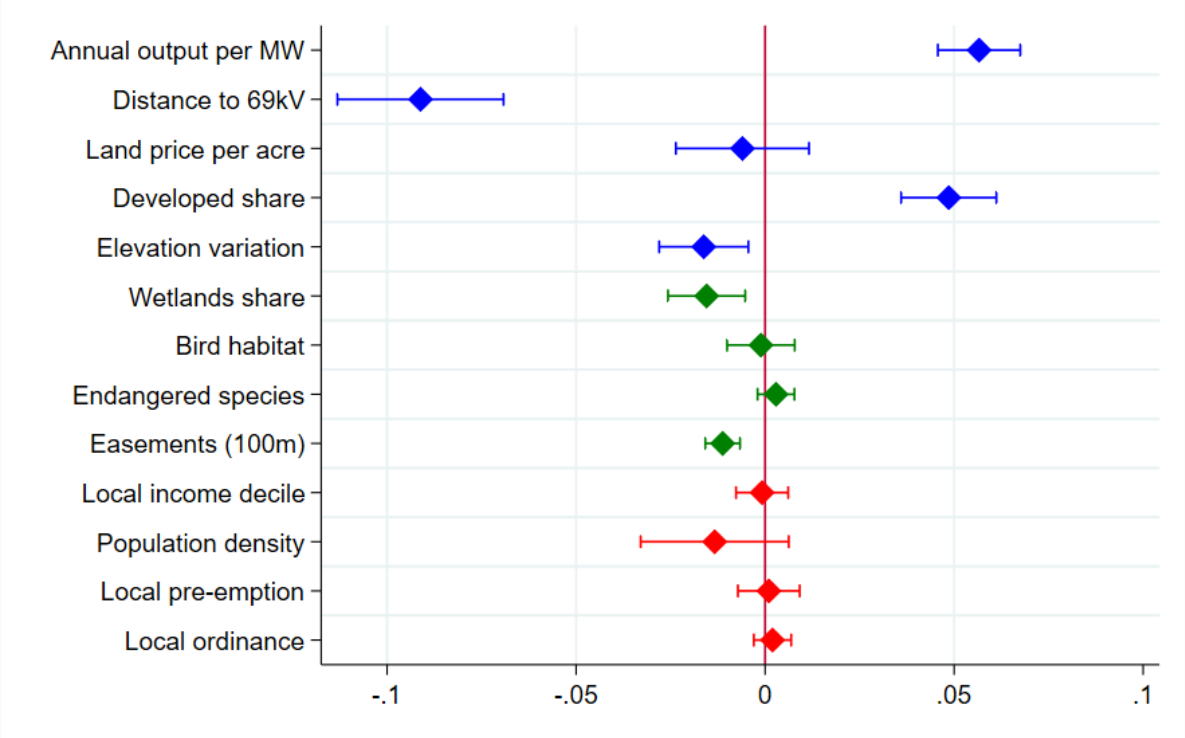
Figure 3: Capacity Factors: Queue Projects vs. Potential Sites



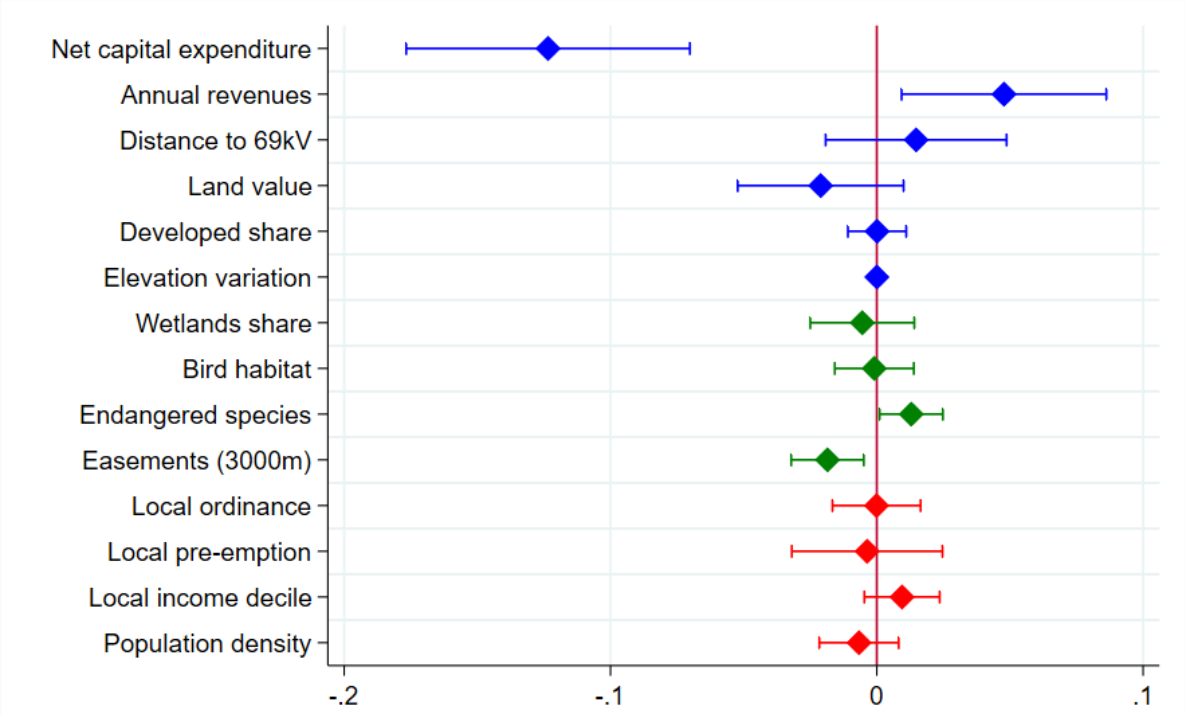
Notes: Maps show simulated capacity factors for wind (top) and solar (bottom) projects. Left panels show queue projects at geocoded locations; right panels show NREL Entity counterfactual sites drawn from the national renewable energy supply curve. Wind capacity factors are derived from PySAM/WTK simulations with vintage-year-specific turbine parameters. Solar capacity factors are from PySAM/PVWatts with year-specific Inverter Loading Ratios. Both are adjusted for 20-year degradation and ISO-specific curtailment.

Figure 4: Wind Projects: Average Marginal Effects

(a) Entry



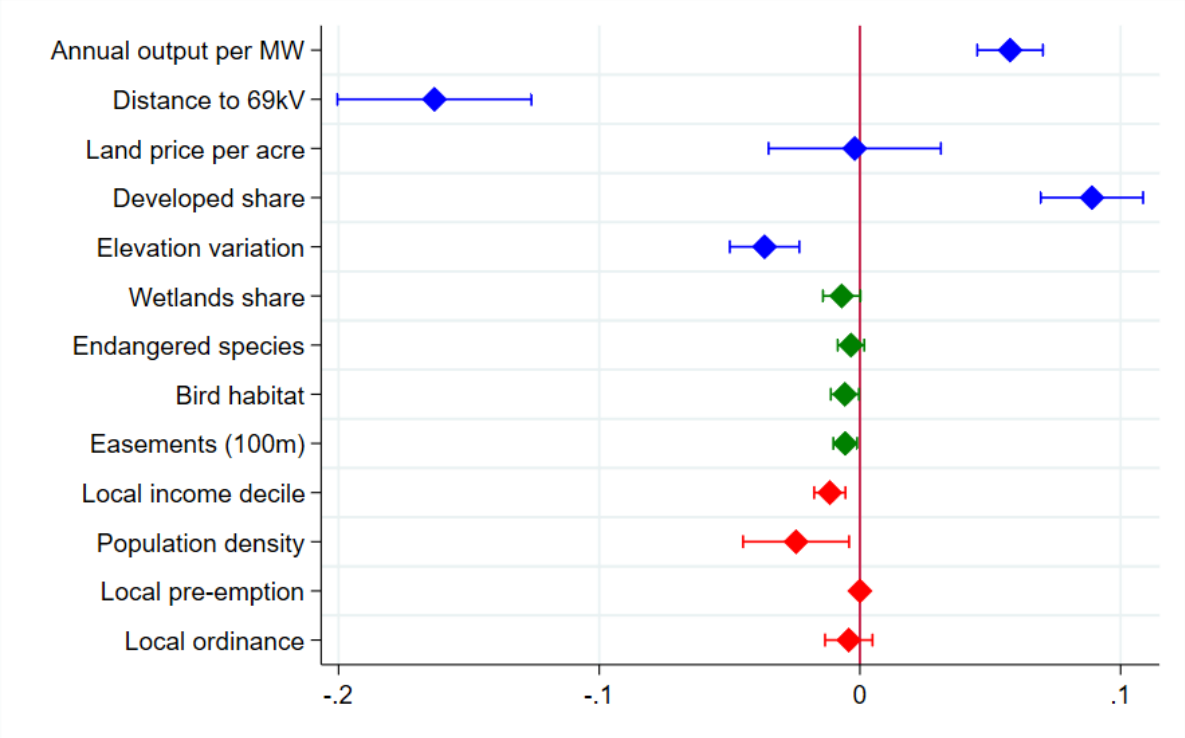
(b) Interconnection



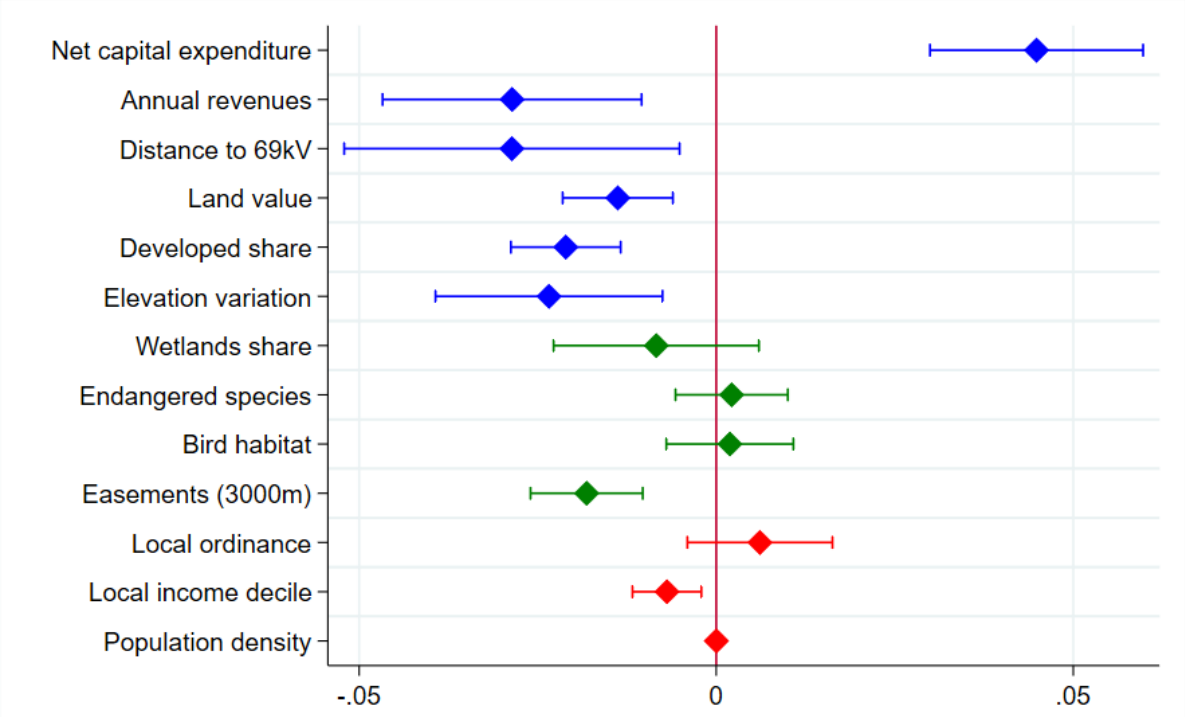
Notes: Panels display average marginal effects from logit models for wind projects. Each point represents the effect of a one-standard-deviation change in the corresponding site attribute. Panel (a) shows the entry model; panel (b) shows the interconnection model with selection correction. Bars show 95% confidence intervals. Standard errors clustered at the state level. ♦ Economic ♦ Land use ♦ Demographic

Figure 5: Solar Projects: Average Marginal Effects

(a) Entry



(b) Interconnection



Notes: Panels display average marginal effects from logit models for solar projects. Each point represents the effect of a one-standard-deviation change in the corresponding site attribute. Panel (a) shows the entry model; panel (b) shows the interconnection model with selection correction. Bars show 95% confidence intervals. Standard errors clustered at the state level.

Table 1: Correlations between conservation metrics, economic profits, and land protections

	Engineering profit (wind)	Engineering profit (solar)	WOTUS regulation	Easements 3000m	Endangered species habitat (ESA)
TNC conservation score (wind)	0.01	.	-0.02	0.02	0.04
TNC conservation score (solar)	.	-0.03	0.02	0.01	0.04
TNC high priority area	0.03	0.02	0.04	0.01	0.03
Wetlands	-0.02	0.03	0.53	0.01	0.04
Species diversity	-0.01	0.00	0.00	0.00	0.04
Bird habitat	0.06	0.02	0.10	0.01	0.06
Observations	55,530	67,425	123,067	123,067	123,067

Notes: Table reports pairwise correlation coefficients. Engineering profit is the calibrated NPV measure using PySAM. Conservation metrics are measured at the gridcell level.

Table 2: Summary Statistics: Wind Projects

	Potential Entrants	Entrants	Interconnection
Economic			
Annual GWh per MW	1.93	2.24	2.32
	(0.59)	(0.52)	(0.48)
Annual revenues	25.86	27.90	24.61
	(36.34)	(33.55)	(20.49)
Distance to 69kV	10.05	3.92	3.60
	(12.25)	(5.91)	(5.50)
Land cost per acre	13,669.54	12,158.40	12,240.62
	(33,240.86)	(22,771.87)	(22,446.40)
Property tax	67.37	58.00	46.43
	(318.29)	(194.02)	(140.24)
Elevation variation	50.89	31.19	28.38
	(66.60)	(40.36)	(39.33)
Developed share	0.07	0.19	0.17
	(0.15)	(0.26)	(0.24)
Land use			
Wetlands share	0.07	0.05	0.04
	(0.16)	(0.10)	(0.09)
Bird habitat	0.09	0.06	0.05
	(0.29)	(0.24)	(0.23)
Endangered species	0.01	0.01	0.02
	(0.11)	(0.12)	(0.14)
Easement acreage (100m)	0.13	0.03	0.01
	(1.02)	(0.45)	(0.22)
Easement acreage (3000m)	122.01	66.49	39.67
	(565.40)	(375.69)	(173.77)
TNC conservation score	6.40	4.77	4.44
	(4.75)	(3.76)	(3.64)
Demographic			
Population density	47.27	130.22	101.12
	(269.03)	(544.52)	(273.80)
Average income decile	4.56	4.72	4.83
	(1.97)	(1.82)	(1.80)
Local pre-emption	0.02	0.03	0.07
	(0.15)	(0.17)	(0.25)
Local ordinance	0.06	0.06	0.14
	(0.23)	(0.24)	(0.35)
N	53,525	5,419	1,589

Mean values; standard deviations in parentheses

Table 3: Summary Statistics: Solar Projects

	Potential Entrants	Entrants	Interconnection
Economic			
Annual GWh per MW	2.12	2.10	2.08
	(0.29)	(0.30)	(0.28)
Annual revenues	15.73	14.24	17.03
	(21.40)	(22.06)	(21.49)
Distance to 69kV	7.73	2.81	2.38
	(10.79)	(5.30)	(4.38)
Land cost per acre	17,346.17	24,455.84	22,785.97
	(41,000.23)	(55,686.07)	(49,721.91)
Property tax	161.72	110.90	125.38
	(516.28)	(440.68)	(540.64)
Elevation variation	40.99	28.15	23.10
	(57.50)	(38.38)	(32.51)
Developed share	0.11	0.24	0.23
	(0.19)	(0.28)	(0.27)
Land use			
Wetlands share	8.41	7.24	6.98
	(17.56)	(12.31)	(11.84)
Endangered species	0.01	0.01	0.01
	(0.14)	(0.14)	(0.13)
Bird habitat	0.09	0.07	0.07
	(0.29)	(0.27)	(0.26)
Easement acreage (100m)	0.14	0.09	0.06
	(1.03)	(0.79)	(0.61)
Easement acreage (3000m)	137.67	146.53	121.67
	(569.60)	(461.23)	(395.40)
TNC conservation score	11.94	7.86	7.22
	(14.11)	(7.94)	(7.68)
Demographic			
Population density	67.01	155.81	144.97
	(259.29)	(375.58)	(352.60)
Average income decile	4.57	4.63	4.64
	(1.88)	(1.63)	(1.63)
Local pre-emption	0.01	0.06	0.08
	(0.12)	(0.25)	(0.28)
Local ordinance	0.10	0.09	0.12
	(0.31)	(0.29)	(0.33)
N	71,232	16,064	6,344

Mean values; standard deviations in parentheses

Table 4: Entry Model: Wind Projects (Average Marginal Effects)

	(1)	(2)	(3)	(4)	(5)	(6)
Annual output per MW	0.057**	0.057**	0.057**	0.057**	0.057**	0.051**
	(0.004)	(0.004)	(0.004)	(0.004)	(0.006)	(0.004)
Distance to 69kV	-0.094**	-0.094**	-0.094**	-0.093**	-0.091**	-0.087**
	(0.009)	(0.009)	(0.009)	(0.009)	(0.011)	(0.009)
Land price per acre	-0.038**	-0.038**	-0.007	-0.007	-0.006	-0.004
	(0.004)	(0.004)	(0.007)	(0.007)	(0.009)	(0.006)
Share of land developed	0.041**	0.041**	0.042**	0.041**	0.049**	0.047**
	(0.002)	(0.002)	(0.002)	(0.002)	(0.006)	(0.005)
Elevation variation	-0.014*	-0.014**	-0.015**	-0.016**	-0.016**	0.005
	(0.005)	(0.005)	(0.005)	(0.005)	(0.006)	(0.006)
Wetlands share				-0.015**	-0.015**	-0.014**
				(0.004)	(0.005)	(0.004)
Bird habitat				-0.001	-0.001	0.002
				(0.004)	(0.005)	(0.004)
Endangered species				0.003	0.003	0.004
				(0.003)	(0.002)	(0.003)
Easements (100m)				-0.011**	-0.011**	-0.011**
				(0.003)	(0.002)	(0.003)
Local income decile					-0.001	-0.002
					(0.004)	(0.004)
Local population density					-0.013	-0.013
					(0.010)	(0.007)
Local pre-emption					0.001	0.000
					(0.004)	(0.002)
Local ordinance					0.002	0.001
					(0.003)	(0.002)
Observations	53,399	53,399	52,964	52,964	52,964	52,964
Mean Dep. Var.	0.101	0.101	0.102	0.102	0.102	0.102
AIC	28599.27	28593.55	28444.70	28334.92	28274.28	27895.80
Year FE	No	Yes	Yes	Yes	Yes	Yes
ISO Period FE	Yes	Yes	Yes	Yes	Yes	Yes
Property tax controls	No	No	Yes	Yes	Yes	Yes
Land use controls	No	No	No	No	No	Yes

Clustered (state) standard errors in parentheses. All variables standardized. Land use controls in col. (6) not shown. * p<0.05, ** p<0.01

Table 5: Interconnection Model: Wind Projects (Average Marginal Effects)

	(1)	(2)	(3)	(4)	(5)	(6)
Net capital expenditure	-0.18**	-0.13**	-0.19**	-0.13**	-0.18**	-0.18**
	(0.03)	(0.03)	(0.03)	(0.03)	(0.03)	(0.03)
Annual revenues	0.08**	0.05*	0.08**	0.05*	0.08**	0.08**
	(0.02)	(0.02)	(0.02)	(0.02)	(0.02)	(0.02)
Distance to 69kV	0.02	0.02	0.02	0.02	0.02	0.03
	(0.02)	(0.02)	(0.02)	(0.02)	(0.02)	(0.02)
Land value	-0.01	-0.02	0.01	0.00	0.01	0.01
	(0.02)	(0.02)	(0.02)	(0.02)	(0.02)	(0.02)
Share of land developed	-0.00	-0.00	-0.00	-0.00	0.00	0.01
	(0.00)	(0.00)	(0.00)	(0.00)	(0.01)	(0.01)
Elevation variation	0.00	-0.00	-0.00	0.00	0.00	0.00
	(0.00)	(0.00)	(0.00)	(0.00)	(0.00)	(0.00)
Selection correction	-0.00	-0.00	-0.00	-0.00	-0.00	-0.00
	(0.00)	(0.00)	(0.00)	(0.00)	(0.00)	(0.00)
Wetlands share				-0.00	-0.00	0.01
				(0.01)	(0.01)	(0.01)
Bird habitat				-0.00	-0.00	-0.00
				(0.01)	(0.01)	(0.01)
Endangered species				0.01	0.01	0.01
				(0.01)	(0.01)	(0.01)
Easements (3000m)				-0.02*	-0.02*	-0.02*
				(0.01)	(0.01)	(0.01)
Local income decile					0.01	0.01
					(0.01)	(0.01)
Local population density					-0.01	-0.01
					(0.01)	(0.01)
Local pre-emption					-0.00	-0.00
					(0.02)	(0.02)
Local ordinance					0.00	0.00
					(0.01)	(0.01)
Observations	5,046	5,046	5,038	5,038	5,038	5,038
Mean Dep. Var.	0.25	0.25	0.25	0.25	0.25	0.25
AIC	4,982	4,918	4,978	4,909	4,975	4,968
ISO Period FE	Yes	Yes	Yes	Yes	Yes	Yes
Year FE	No	Yes	No	No	No	No
Property tax controls	No	No	Yes	Yes	Yes	Yes
Land use controls	No	No	No	No	No	Yes

Clustered (state) standard errors in parentheses. All variables standardized. Land use controls in col. (6) not shown. * p<0.05, ** p<0.01

Table 6: Entry Model: Solar Projects (Average Marginal Effects)

	(1)	(2)	(3)	(4)	(5)	(6)
Annual output per MW	0.059**	0.061**	0.061**	0.060**	0.058**	0.052**
	(0.006)	(0.007)	(0.006)	(0.006)	(0.006)	(0.006)
Distance to 69kV	-0.176**	-0.176**	-0.176**	-0.174**	-0.163**	-0.157**
	(0.019)	(0.019)	(0.019)	(0.019)	(0.019)	(0.019)
Land price per acre	-0.020*	-0.020*	-0.007	-0.007	-0.002	-0.001
	(0.008)	(0.008)	(0.016)	(0.016)	(0.017)	(0.016)
Share of land developed	0.076**	0.076**	0.077**	0.075**	0.089**	0.084**
	(0.004)	(0.004)	(0.004)	(0.004)	(0.010)	(0.010)
Elevation variation	-0.037**	-0.037**	-0.038**	-0.039**	-0.037**	-0.019**
	(0.007)	(0.007)	(0.007)	(0.007)	(0.007)	(0.007)
Wetlands share				-0.007	-0.007	-0.011*
				(0.004)	(0.004)	(0.004)
Endangered species				-0.004	-0.003	-0.003
				(0.003)	(0.003)	(0.003)
Bird habitat				-0.006*	-0.006*	-0.001
				(0.003)	(0.003)	(0.003)
Easements (100m)				-0.006**	-0.006*	-0.006**
				(0.002)	(0.002)	(0.002)
Local income decile					-0.012**	-0.014**
					(0.003)	(0.003)
Local population density					-0.024*	-0.023*
					(0.010)	(0.010)
Local pre-emption					0.000	0.000
					(.)	(.)
Local ordinance					-0.004	-0.005
					(0.005)	(0.005)
Observations	71,775	71,775	71,302	71,302	70,263	70,263
Mean Dep. Var.	0.226	0.226	0.228	0.228	0.216	0.216
AIC	59108.55	59077.13	58831.44	58771.95	56343.06	55837.55
ISO Period FE	Yes	Yes	Yes	Yes	Yes	Yes
Year FE	No	Yes	Yes	Yes	Yes	Yes
Property tax controls	No	No	Yes	Yes	Yes	Yes
Land use controls	No	No	No	No	No	Yes

Clustered (state) standard errors in parentheses. All variables standardized. Land use controls in col. (6) not shown. * p<0.05, ** p<0.01

Table 7: Interconnection Model: Solar Projects (Average Marginal Effects)

	(1)	(2)	(3)	(4)	(5)	(6)
Net capital expenditure	0.031**	0.001	0.039**	-0.001	0.038**	0.009
	(0.010)	(0.009)	(0.009)	(0.009)	(0.009)	(0.009)
Annual revenues	-0.010	0.035**	-0.018	0.036**	-0.017	0.022*
	(0.013)	(0.011)	(0.011)	(0.011)	(0.011)	(0.011)
Distance to 69kV	-0.048**	-0.024	-0.028*	-0.023	-0.027	-0.026
	(0.015)	(0.014)	(0.014)	(0.014)	(0.014)	(0.014)
Land value	-0.014**	-0.012**	-0.013**	-0.013**	-0.013**	-0.013**
	(0.004)	(0.005)	(0.004)	(0.004)	(0.004)	(0.005)
Share of land developed	-0.015**	-0.014**	-0.015**	-0.014**	-0.015**	-0.018**
	(0.004)	(0.004)	(0.004)	(0.004)	(0.004)	(0.005)
Elevation variation	-0.063**	-0.020*	-0.022*	-0.021*	-0.023*	-0.020*
	(0.011)	(0.009)	(0.009)	(0.009)	(0.009)	(0.009)
Selection correction	0.000	0.000	0.000	-0.000	0.000	0.000
	(0.000)	(0.000)	(0.000)	(0.000)	(0.000)	(0.000)
Wetlands share				-0.010	-0.011	-0.009
				(0.008)	(0.008)	(0.008)
Endangered species				0.002	0.002	0.003
				(0.005)	(0.005)	(0.005)
Bird habitat				0.002	0.002	0.001
				(0.006)	(0.006)	(0.005)
Easements (3000m)				-0.018**	-0.017**	-0.019**
				(0.005)	(0.005)	(0.005)
Local income decile						-0.006*
						(0.003)
Local population density						0.000
						(0.000)
Local pre-emption						0.000
						(.)
Local ordinance						-0.052
						(0.052)
Observations	13,215	13,165	13,165	13,165	13,165	12,717
Mean Dep. Var.	0.341	0.341	0.341	0.341	0.341	0.341
AIC	15,595	14,748	14,583	14,728	14,565	14,186
ISO Period FE	No	Yes	Yes	Yes	Yes	Yes
Year FE	Yes	No	Yes	No	Yes	No
Property tax controls	No	Yes	Yes	Yes	Yes	Yes
Land use controls	No	No	No	No	No	Yes

Clustered (state) standard errors in parentheses. All variables standardized. * p<0.05, ** p<0.01

References

Aldy, Joseph E, Todd D Gerarden, and Richard L Sweeney. 2023. "Investment versus output subsidies: Implications of alternative incentives for wind energy." *Journal of the Association of Environmental and Resource Economists* 10 (4): 981–1018.

Aronoff, Daniel, and Will Rafey. 2026. "Conservation Priorities and Environmental Offsets: Markets for Florida Wetlands." *American Economic Review*.

Auffhammer, Maximilian, Maya Duru, Edward Rubin, and David L. Sunding. 2020. "The Economic Impact of Critical-Habitat Designation: Evidence from Vacant-Land Transactions." *Land Economics* 96:188–206.

Borenstein, Severin. 2012. "The private and public economics of renewable electricity generation." *Journal of Economic Perspectives* 26 (1): 67–92.

Davis, Lucas W, Catherine Hausman, and Nancy L Rose. 2023. "Transmission impossible? Prospects for decarbonizing the US grid." *Journal of Economic Perspectives* 37 (4): 155–180.

Deschenes, Olivier, Christopher Malloy, and Gavin McDonald. 2023. "Causal effects of Renewable Portfolio Standards on renewable investments and generation: The role of heterogeneity and dynamics." *Resource and Energy Economics* 75:101393.

Druckenmiller, Hannah, Joseph Shapiro, and Charles Taylor. 2026. *Paving the Swamp: Consequences of Land Use Regulation Under the Clean Water Act.* Technical report.

Fell, Harrison, Daniel T Kaffine, and Kevin Novan. 2021. "Emissions, transmission, and the environmental value of renewable energy." *American Economic Journal: Economic Policy* 13 (2): 241–272.

Ferris, Ann E, and Eyal G Frank. 2021. "Labor market impacts of land protection: The Northern Spotted Owl." *Journal of Environmental Economics and Management* 109:102480.

Frank, Eyal G, Maximilian Auffhammer, David McLaughlin, Elisheba Spiller, and David L Sunding. 2025. *The Cost of Species Protection: The Land Market Impacts of the Endangered Species Act.* Technical report. National Bureau of Economic Research.

Greenhill, Simon, Hannah Druckenmiller, Sherrie Wang, David A Keiser, Manuela Girotto, Jason K Moore, Nobuhiro Yamaguchi, Alberto Todeschini, and Joseph S Shapiro. 2024. "Machine learning predicts which rivers, streams, and wetlands the Clean Water Act regulates." *Science* 383 (6681): 406–412.

Grupp, Tristan, Prakash Mishra, Mathias Reynaert, and Arthur A van Benthem. 2023. *An evaluation of protected area policies in the european union.* Technical report. National Bureau of Economic Research.

Hamilton, Healy, Regan L Smyth, Bruce E Young, Timothy G Howard, Christopher Tracey, Sean Breyer, D Richard Cameron, Anne Chazal, Amy K Conley, Charlie Frye, et al. 2022. "Increasing taxonomic diversity and spatial resolution clarifies opportunities for protecting US imperiled species." *Ecological Applications* 32 (3): e2534.

Harstad, Bård. 2023. "The conservation multiplier." *Journal of Political Economy* 131 (7): 1731–1771.

Jarvis, Stephen. 2021. "The economic costs of NIMBYism: evidence from renewable energy projects."

Jaureguiberry, Pedro, Nicolas Titeux, Martin Wiemers, Diana E Bowler, Luca Coscieme, Abigail S Golden, Carlos A Guerra, Ute Jacob, Yasuo Takahashi, Josef Settele, et al. 2022. "The direct drivers of recent global anthropogenic biodiversity loss." *Science advances* 8 (45): eabm9982.

Johnston, Sarah, Yifei Liu, and Chenyu Yang. 2023. *An Empirical Analysis of the Interconnection Queue.* Technical report. National Bureau of Economic Research.

Jones, Wu, Leslie, Hise, Fargione, Johnson, Hiltibran, Kalies, Cohen, and Williams. 2023. "Power of Place - National - Environmental and social impact score datasets," https://doi.org/10.5281/zenodo.7878144. https://doi.org/10.5281/zenodo.7878144.

Kashner, Zane. 2026. "Building with Externalities: Local Governments and Wind Farms." Working paper, Stanford Graduate School of Business.

Klein, Ezra, and Derek Thompson. 2025. *Abundance: On Freedom, Prosperity, and the Best Ideas for Moving American Life Forward.* Avid Reader Press.

Larson, Eric. 2020. *Net-zero America: Potential pathways, infrastructure, and impacts.* Princeton University.

Lopez, Anthony, Wesley Cole, Brian Sergi, Aaron Levine, Jesse Carey, Cailee Mangan, Trieu Mai, Travis Williams, Pavlo Pinchuk, and Jianyu Gu. 2023. "Impact of siting ordinances on land availability for wind and solar development." *Nature Energy* 8:1034–1043. https://doi.org/10.1038/s41560-023-01319-3.

Newbold, Tim, Lawrence N Hudson, Samantha LL Hill, Sara Contu, Igor Lysenko, Rebecca A Senior, Luca Börger, Dominic J Bennett, Argyrios Choimes, Ben Collen, et al. 2015. "Global effects of land use on local terrestrial biodiversity." *Nature* 520 (7545): 45–50.

Rand, Joseph, and Ben Hoen. 2017. "Thirty years of North American wind energy acceptance research: What have we learned?" *Energy research & social science* 29:135–148.

Rand, Joseph, Rose Strauss, Will Gorman, Joachim Seel, Julie Mulvaney Kemp, Seongeun Jeong, Dana Robson, and Ryan H Wiser. 2024. "Queued up: Characteristics of power plants seeking transmission interconnection as of the end of 2023."

Reynaert, Mathias, Eduardo Souza-Rodrigues, and Arthur A. van Benthem. 2024. "The Environmental Impacts of Protected Area Policy." *Regional Science and Urban Economics* 107:103968. https://doi.org/10.1016/j.regsciurbeco.2023.103968.

Shawhan, Daniel L., Kathryne Cleary, Christoph Funke, and Steven Witkin. 2020. "Your Money or Your Wildlife: Environmental and Economic Tradeoffs from Solar Siting Restrictions in Texas." Conference presentation, Resources for the Future.

Susskind, Lawrence, Jungwoo Chun, Alexander Gant, Chelsea Hodgkins, Jessica Cohen, and Sarah Lohmar. 2022. "Sources of opposition to renewable energy projects in the United States." *Energy Policy* 165:112922. ISSN: 0301-4215. https://doi.org/https://doi.org/10.1016/j.enpol.2022.112922. https://www.sciencedirect.com/science/article/pii/S0301421522001471.

Taylor, Charles A, and Hannah Druckenmiller. 2022. "Wetlands, Flooding, and the Clean Water Act." *American Economic Review* 112 (4): 1334–63.

Uebelhor, Emma, Olivia Hintz, and Eli Gold. 2021. *Inventory of State Wind Property Tax Treatments.* Working Paper 55. Center for Local, State, and Urban Policy (CLOSUP), University of Michigan.

Voorheis, John, Jonathan Colmer, Kendall Houghton, Eva Lyubich, Mary Munro, Cameron Scalera, and Jennifer Withrow. 2024. *The Privacy-Protected Gridded Environmental Impacts Frame.* Working Paper CES-WP-24-74. U.S. Census Bureau.

Wells, Jeffrey V., Daniel K. Niven, and John Cecil. 2005. "The Important Bird Areas Program in the United States: Building a Network of Sites for Conservation, State by State." In *Bird Conservation Implementation and Integration in the Americas: Proceedings of the Third International Partners in Flight Conference,* edited by C. John Ralph and Terrell D. Rich, 1265–1269. Gen. Tech. Rep. PSW-GTR-191. USDA Forest Service.

Williams, James H, Ryan A Jones, Ben Haley, Gabe Kwok, Jeremy Hargreaves, Jamil Farbes, and Margaret S Torn. 2021. "Carbon-neutral pathways for the United States." *AGU advances* 2 (1): e2020AV000284.

Winikoff, Justin B, and Dominic P Parker. 2024. "Farm size, spatial externalities, and wind energy development." *American Journal of Agricultural Economics* 106 (4): 1518–1543.

Wu, Grace C, Ryan A Jones, Emily Leslie, James H Williams, Andrew Pascale, Erica Brand, Sophie S Parker, Brian S Cohen, Joseph E Fargione, Julia Souder, et al. 2023. "Minimizing habitat conflicts in meeting net-zero energy targets in the western United States." *Proceedings of the National Academy of Sciences* 120 (4): e2204098120.

A Appendix

A.1 Data Appendix

Capacity factor simulation. Capacity factors for wind projects are derived from pre-computed PySAM simulations using NREL's Wind Toolkit (WTK) mesoscale weather data for a single representative meteorological year (2012). Each simulation uses vintage-year-specific turbine parameters—hub height, rotor diameter, and power curve—reflecting the representative technology available at the time a project entered the queue. Each project is matched to the nearest cached simulation result by Euclidean distance on (lat, lon). Capacity factors for solar projects are computed from NREL's PySAM PVWatts model run on Typical Meteorological Year (TMY) weather files from the National Solar Radiation Database (NSRDB) at 0.25-degree grid resolution across CONUS. TMY files represent a synthetic composite of typical weather conditions rather than a single calendar year. Key parameters include single-axis tracking, standard crystalline silicon modules, and year-specific Inverter Loading Ratios (ILR) ranging from 1.10 (2009) to 1.34 (2020), reflecting the industry trend toward DC oversizing relative to AC inverter capacity. For both technologies, base-year generation is adjusted for 20-year average degradation (0.5%/year) and ISO-specific curtailment rates drawn from LBNL's annual technology reports. Historical curtailment rates are available for CAISO, ERCOT, and SPP; CAISO rates are applied to the broader West; national averages are used for other ISOs. Projected curtailment extends the trailing 5-year average. Expected annual generation is $E_i = CF_i \times MW_i \times 8{,}760$ hours, adjusted by the curtailment-degradation factor.

Expected revenues. Renewable energy project developers typically sign long-term Power Purchase Agreements (PPAs) prior to construction. Under a PPA, an offtaker agrees to purchase the project's electricity at a contracted price per megawatt-hour. These agreements allocate price, volume, and regulatory risk between the buyer and developer and provide the predictable revenue stream necessary to obtain project financing. These are typically 15–20 year contracts that include both the value of electricity generation and associated renewable energy credits (RECs) in states with renewable energy portfolio requirements. Contract prices embed expectations about future wholesale electricity market prices and REC prices. PPA data collected by Lawrence Berkeley National Laboratory (LBNL) include contract execution dates, nominal prices, and contracted capacities. We aggregate these contract prices using capacity-weighted averages for each ISO-year for wind and solar projects, respectively. For each project and queue entry year, we estimate the value of federal tax credits under the Investment Tax Credit (ITC) and Production Tax Credit (PTC). The PTC provides

an inflation-adjusted per-kWh payment over the first 10 years of generation. We compute annualized PTC values using curtailment- and degradation-adjusted expected generation, applying the statutory rate corresponding to the project's construction year in 2023 dollars. The ITC provides a lump-sum credit equal to a percentage of capital expenditure—30% for solar throughout most of our sample period, and 30% for wind during 2009–2012 and 2025–2034 (under the IRA extension). To facilitate comparison with the PTC, we convert the lump-sum ITC into an equivalent annual payment using a capital recovery factor ($r = 0.02$, $n = 10$ years). We assume that developers select the tax credit option yielding the larger annualized value. We also model the depreciation tax shield from 5-year Modified Accelerated Cost Recovery System (MACRS) depreciation. PTC-claiming projects depreciate full CapEx; ITC-claiming projects depreciate CapEx minus half the credit claimed, per Section 50(c) of the Internal Revenue Code. We compute the NPV of the MACRS schedule at a 6% discount rate, multiply by a 21% corporate tax rate, and annualize over a 20-year project life. We do not model bonus depreciation. All financial variables are computed at three queue-entry offsets ($t = 0, 2, 5$ years), representing scenarios where the project begins operation immediately, or with a 2- or 5-year construction delay.

Development costs. We measure the Euclidean distance from each site to the nearest high-voltage transmission line ($\geq$69 kV) using the Homeland Infrastructure Foundation-Level Data (HIFLD) national transmission lines dataset. Because the transmission network expands over time, we construct time-varying distance measures using annual snapshots of the network from 1985 to 2023 (Preonas, Sweeney, and Taylor 2026). Each project is assigned the distance corresponding to the network configuration two years after queue entry, reflecting planned near-term transmission expansion relevant to the project's interconnection timeline. We also compute distance to higher-voltage lines ($\geq$345 kV) and to the nearest substation as alternative measures. We measure land acquisition costs using property transaction data from CoreLogic. For each project site, we identify the 10 nearest arm's-length land sales occurring within one year of the project's queue entry date and compute the median sale price per acre. This nearest-neighbor approach captures local land market conditions while smoothing over idiosyncratic transactions. We estimate a project's total land cost as the product of the per-acre price, the project's capacity, and a technology-specific land-use intensity factor (80 acres per MW for wind, 7 acres per MW for solar), assuming that developers purchase approximately 2% of the project footprint and lease the remainder. We also construct property tax variables from CoreLogic records. Effective tax rates are computed as the ratio of tax amount to sale price at the parcel level, then filled hierarchically—with county and state medians where parcel-level data are unavailable—and rasterized for extraction at project locations. We winsorize the resulting rates. Following Uebelhor et al.

(2021) and Kashner (2026), we classify states into three categories: those offering property tax exemptions for renewable energy (14 states), those allowing negotiated tax abatements (12 states), and those applying standard property tax assessment. Our primary tax variable is the product of the effective tax rate and local land price per acre. We interact this measure with an indicator for states applying standard assessment—i.e., states without exemptions or abatements—to capture the additional tax burden faced by projects in those jurisdictions. We construct year-specific capital expenditure estimates by technology type using two complementary sources. For historical years (1998–2023 for wind, 2009–2023 for solar), we use capacity-weighted average installed costs from LBNL's annual technology market reports—a single national $/kW value for each year and technology. For projected years beyond the historical record, we use median CapEx from NREL's Annual Technology Baseline (ATB) under the Moderate scenario, taking the median across all technology classes within each publication year. All values are converted to 2023 dollars.

Site characteristics. We measure terrain roughness as the standard deviation of elevation within a buffer around each project site, extracted from USGS digital elevation model data. We compute land cover shares within a 1000m buffer of each project site using the USGS National Land Cover Database (NLCD) annual 30m rasters, available from 2000 to 2024. Each project is matched to the NLCD layer corresponding to its queue entry year. We extract the share of developed land (NLCD classes 21–24) and wetland (classes 90, 95) as primary controls, with additional land cover categories (forest, cropland) included in some specifications.

Geolocation: Our empirical strategy requires project-level coordinates to measure proximity to conservation lands and other site attributes. The LBNL queue data report a point of interconnection (POI) name, project name, county, and state for each record, but most lack coordinates. We assign locations using a two-stage approach: a tiered algorithmic geocoder that prioritizes matching to known infrastructure, followed by an override cascade that incorporates ISO-specific ground-truth coordinates where available.

The algorithmic stage proceeds through nine tiers. We first extract coordinates embedded in POI text fields. We then match cleaned POI names to the Homeland Infrastructure Foundation-Level Data (HIFLD) national substations database, which contains approximately 20,000 georeferenced substations, using both exact and fuzzy string matching. For records where the Google Geocoding API returns only an approximate location, we snap to the nearest HIFLD substation within 5 km, recovering precise infrastructure coordinates for an additional 2,700 records. For POIs that reference a transmission line (e.g., "Dunkirk–Silver Creek 115 kV Line"), we identify the line endpoints in the HIFLD transmission lines

dataset and assign the midpoint. These infrastructure-based methods yield coordinates for approximately one-third of wind and solar records. For remaining records, we submit structured queries—combining the cleaned POI name, project name, county, and state—to the Google Geocoding API. Google returns metadata that we use to distinguish precise results from cases where the geocoder returns only a county-level match. Records that fail all methods receive the county geographic centroid as a final fallback.

We then apply an override cascade that replaces algorithmic coordinates with ground-truth locations obtained directly from ISOs and federal databases. For PJM, BPA, and MISO, we incorporate GIS coordinates published by each ISO, matched via queue identifiers. For ERCOT, we fuzzy-match project names to coordinates from the ERCOT PERFORM database. For remaining poorly geocoded records, we match CAISO POI names to known substation locations and fuzzy-match project names to operational plant coordinates in the EIA-860 database. These six override sources provide coordinates for 6,146 records (26% of the sample), with PJM alone contributing 4,416. In total, 82% of the 23,853 wind and solar projects receive precise coordinates (infrastructure match, ISO GIS, or address-level Google result), 18% receive a county-level location, and fewer than 1% (137 records) remain unlocated. We classify each record by geolocation method, enabling robustness checks that restrict the sample to precisely located projects.

We validate geolocation accuracy using PJM projects, for which we have independently obtained GIS coordinates (n = 4,413 records, representing 19% of the sample). We compare these reference coordinates against our algorithmic geocoding results—that is, the coordinates our pipeline assigns before the PJM override is applied. Substation-matched records achieve median errors of 4–6 km, Google-geocoded records 8–10 km, and county-level assignments approximately 20 km. Across all methods, the overall median geolocation error is 8.4 km, with 55% of records within 10 km of the reference coordinates. Because county-level assignments could attenuate measured proximity to conservation lands, we verify that our main results are robust to restricting the sample to the 82% of projects with precise coordinates. The PJM validation covers the Mid-Atlantic and parts of the Midwest; error rates may differ in other regions, though the infrastructure-matching methods rely on the same national databases throughout.

Gridcell assignment: Wind and solar projects are processed separately. Each LBNL project is snapped to the nearest analysis gridcell, and gridcell centroids are used in place of project-level coordinates to compute resource economics (based on project year and capacity) and site characteristics (land use, easements, transmission distance). Gridcells may contain multiple LBNL projects to preserve full sample coverage, though analyses can alternatively

restrict to the nearest match only. For potential sites without an observed LBNL project, project year and capacity (MW) are imputed by sampling, with replacement, from the distribution of LBNL projects within the same ISO or market region.

A.2 Conceptual Framework: Proof of Proposition 1

[TODO: Include full proof from conceptual framework. The proof shows that welfare gains $\Delta W(\rho)$ are decreasing in $\rho_{v\pi}$, establishing that ΔW is maximized at $\rho = 0$. The argument proceeds in two parts: (1) the change from site selection $G(\rho)$ is decreasing in ρ under the positive-dependence assumption, and (2) the change in consumer surplus $H(\rho)$ is also decreasing in ρ.]

A.3 Formal derivation of static representation (Stage 1)

[TODO: Include the formal proof that the dynamic application problem with option value $G(z_{i,0})$ is observationally equivalent to a static binary-choice model under assumptions A1–A4.]

A.4 Stage 2 control function details

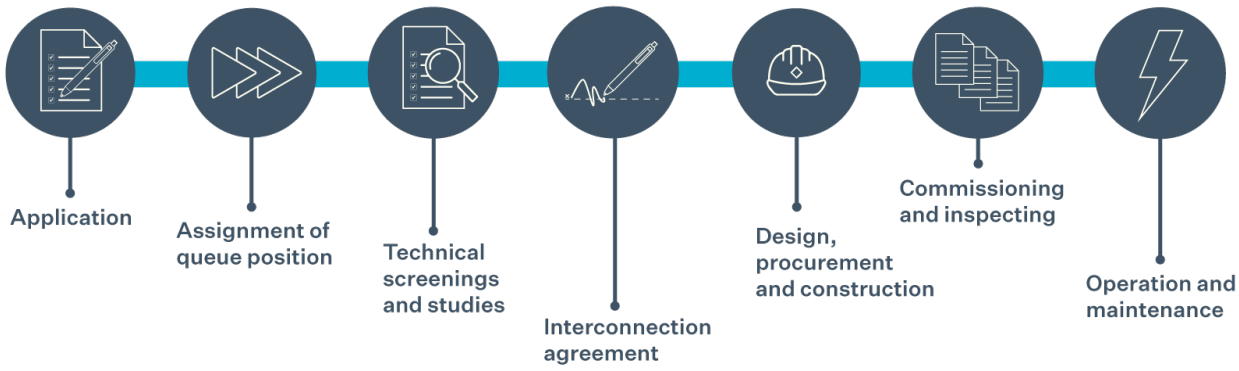
[TODO: Include the formal derivation showing that under A1–A5, the interconnection decision has a static single-index representation with a control function correction for selection.]

A.5 Policy evaluation: money metric and counterfactual details

[TODO: Include the detailed money metric construction, the micro vs. macro decomposition to avoid double counting, the two estimands (conditional-on-entrants and entry-adjusted ex-ante), marginal effects formulas, and the PE+feedback implementation with price and land cost pass-throughs.]

A.6 Additional Figures

Figure 6: Interconnection Queue Process [PRELIMINARY]



Notes: Schematic illustrating the interconnection queue process. Proposed projects must wait in the queue while transmission network operators study grid impacts and assess required network upgrades. Source: LBNL 2025.

Figure 7: Power Purchase Agreement Prices by Region and Technology

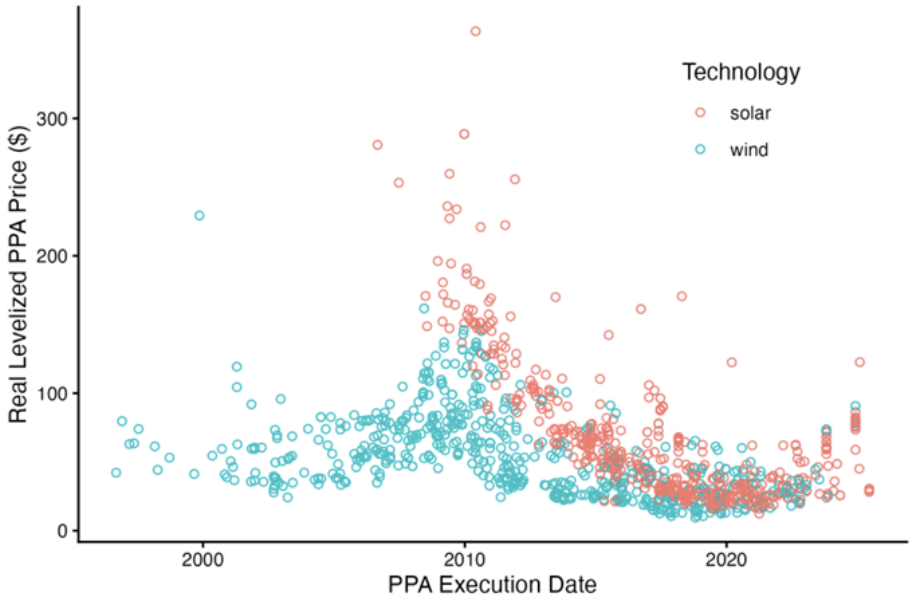
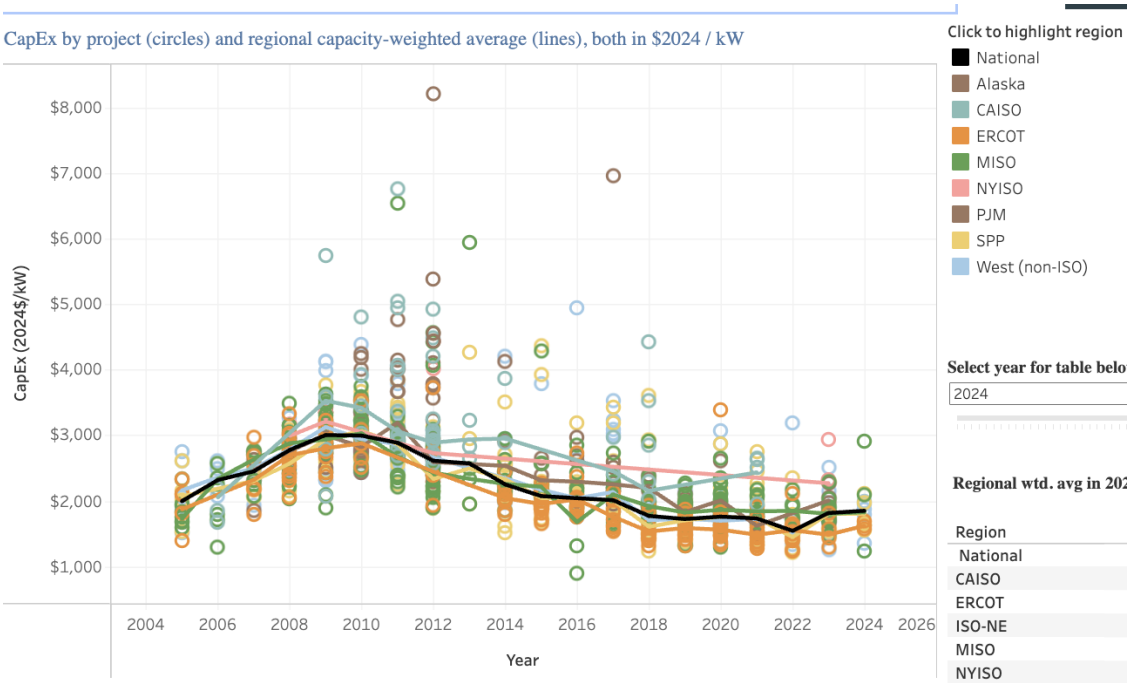


Figure 4: Real Levelized PPA Prices Over Time

Notes: The figure plots real levelized PPA prices by COD. Prices are expressed in 2024 dollars.

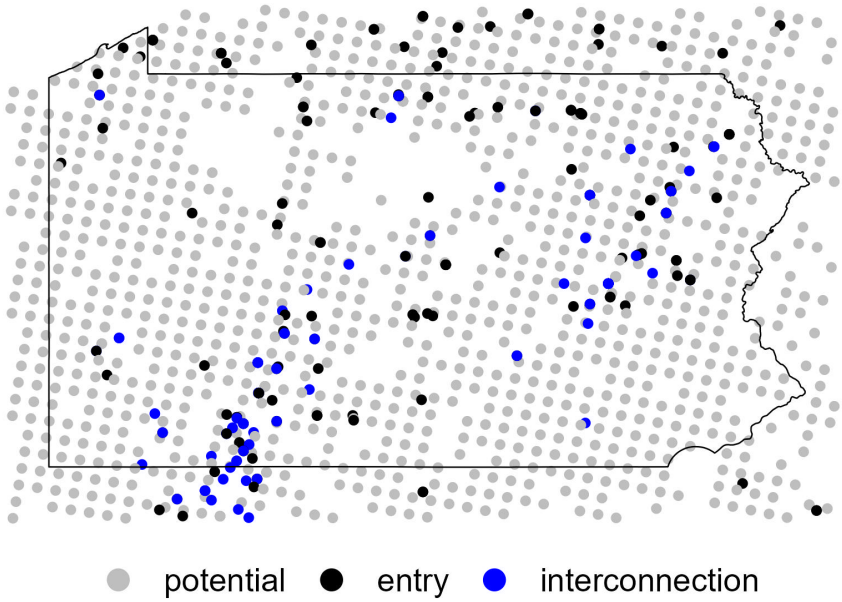
Notes: Figure shows capacity-weighted average PPA prices by ISO-region and technology type over time. PPA data from Lawrence Berkeley National Laboratory.

Figure 8: Capital Expenditure Trends



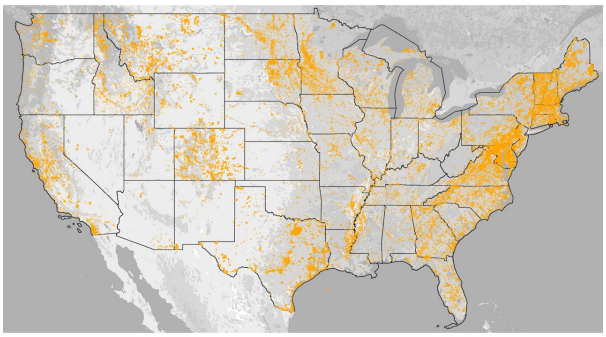
Notes: Figure shows historical and projected capital expenditure per kW by technology type. Historical values from LBNL annual technology market reports; projections from NREL Annual Technology Baseline (Moderate scenario). All values in 2023 dollars.

Figure 9: Illustrative Map of NREL Potential Entrant Sites (Pennsylvania Wind)

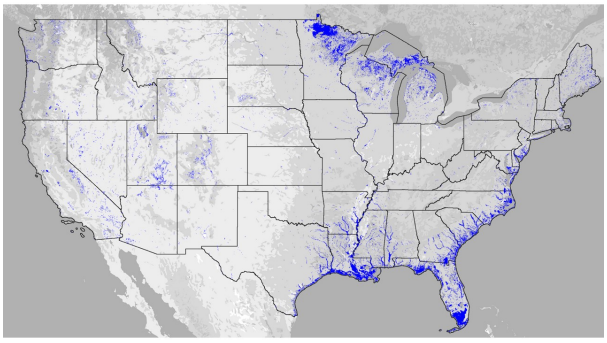


Notes: Map shows NREL supply curve gridcells (gray) and actual queue entrants (blue/black) for wind projects in Pennsylvania. Each NREL gridcell represents a technically viable development site with pre-computed resource characteristics under the "open access" siting regime.

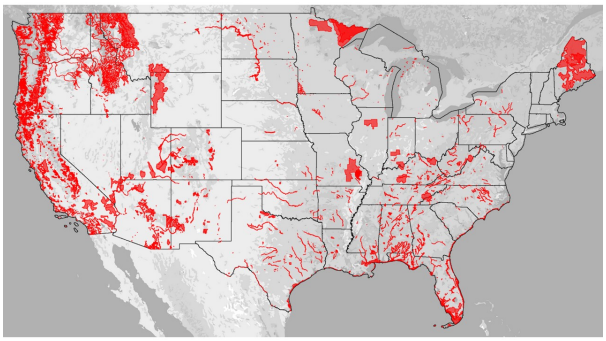
Figure 10: Land Use Restriction Maps



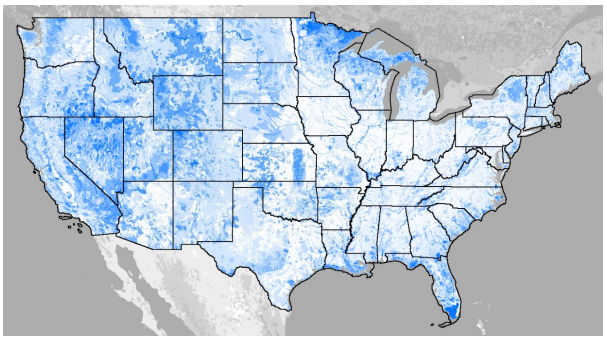
(a) Conservation easements



(b) Wetlands (NWI)



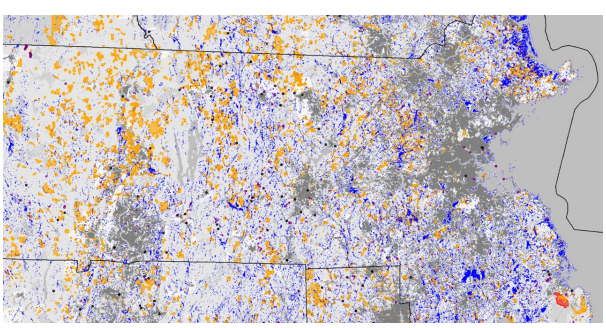
(c) Endangered species critical habitat



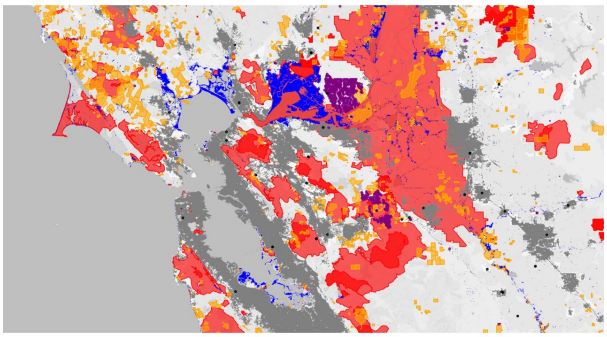
(d) TNC conservation impact scores (wind)

Notes: Maps show the spatial distribution of four categories of land use restrictions and conservation measures. Data from NCED (easements), NWI/USFWS (wetlands), USFWS (critical habitat), and The Nature Conservancy Power of Place initiative (TNC scores).

Figure 11: Regional Detail: Land Use Restrictions and Queued Projects



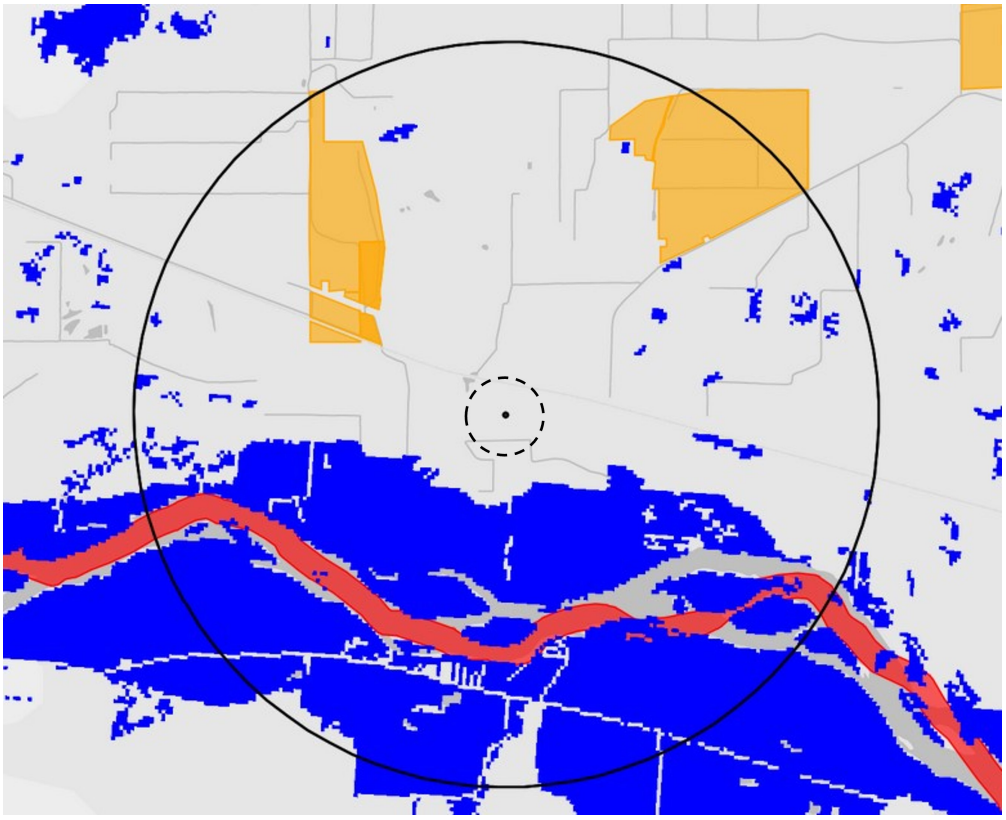
(a) Boston metropolitan area



(b) San Francisco Bay Area

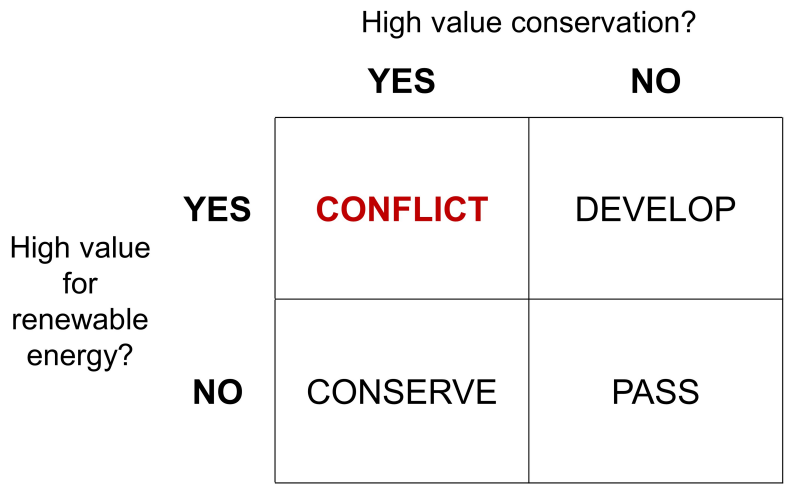
Notes: Detailed views showing the spatial relationship between queued renewable energy projects and conservation lands. Red: critical habitat; blue: wetlands; orange: conservation easements; purple: existing wind/solar; black: projects in queue.

Figure 12: Construction of Land Use Restriction Measures [PRELIMINARY]



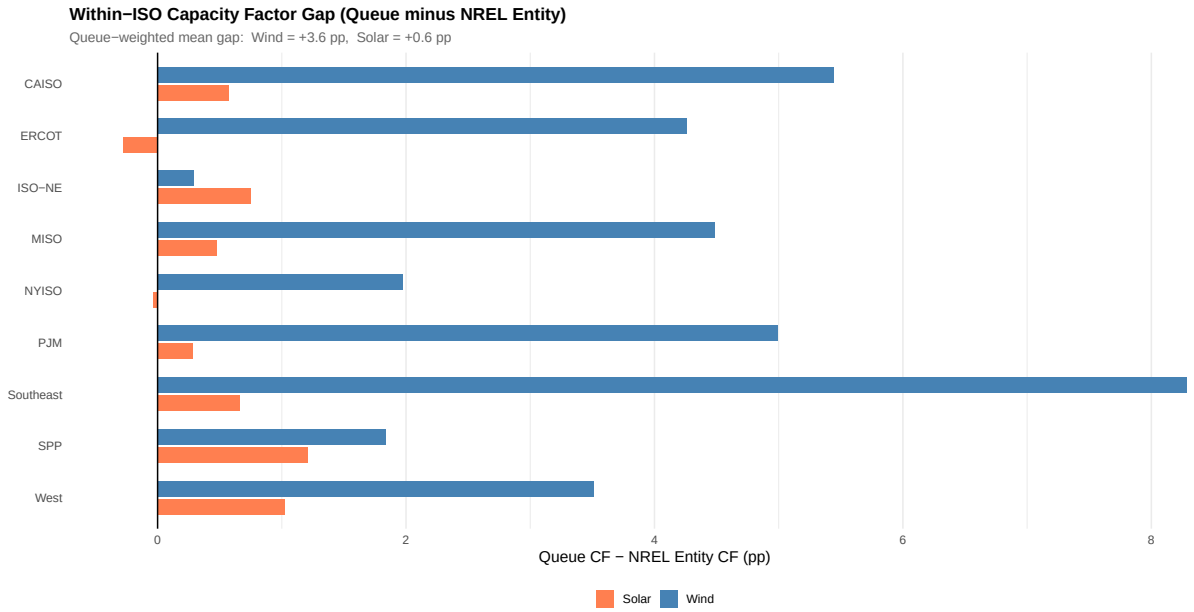
Notes: Example wind project in the interconnection queue near Lewiston, Wisconsin. Black circle is a 3km radius around the project centroid; dashed circle is 100m. Within each buffer, we calculate the area overlapping with land use restrictions: red = critical habitat, blue = wetlands, orange = conservation easements.

Figure 13: Conservation decision matrix



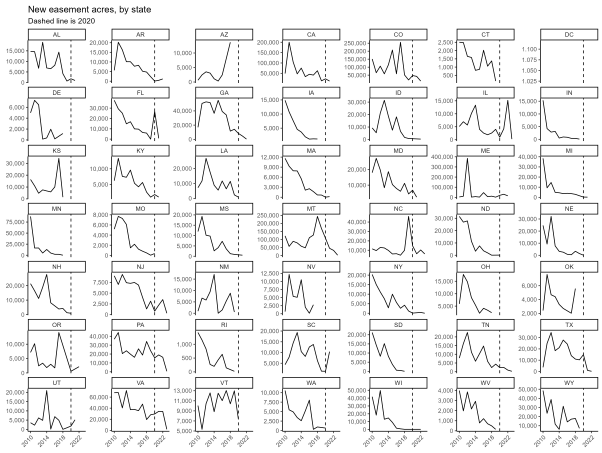
Notes: Framework illustrating the relationship between conservation value and economic potential, and the implied welfare consequences of land use restrictions.

Figure 14: Within-ISO Capacity Factor Gap (Queue minus Counterfactual)

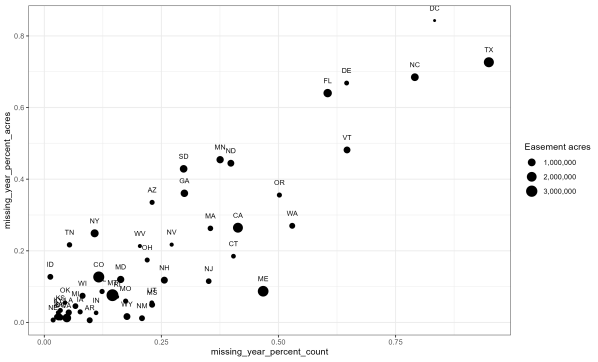


Notes: Bars show the difference in mean capacity factor between queue projects and NREL Entity counterfactual sites within each ISO. Queue-weighted mean gaps are reported in the subtitle. For wind, the within-ISO gap accounts for approximately 77% of the unconditional gap, indicating that developers select superior microsites within their target markets.

Figure 15: Conservation Easement Trends and Data Quality [PRELIMINARY — TO BE UPDATED WITH LATEST NRCS/TNC/STATE ADDITIONS]



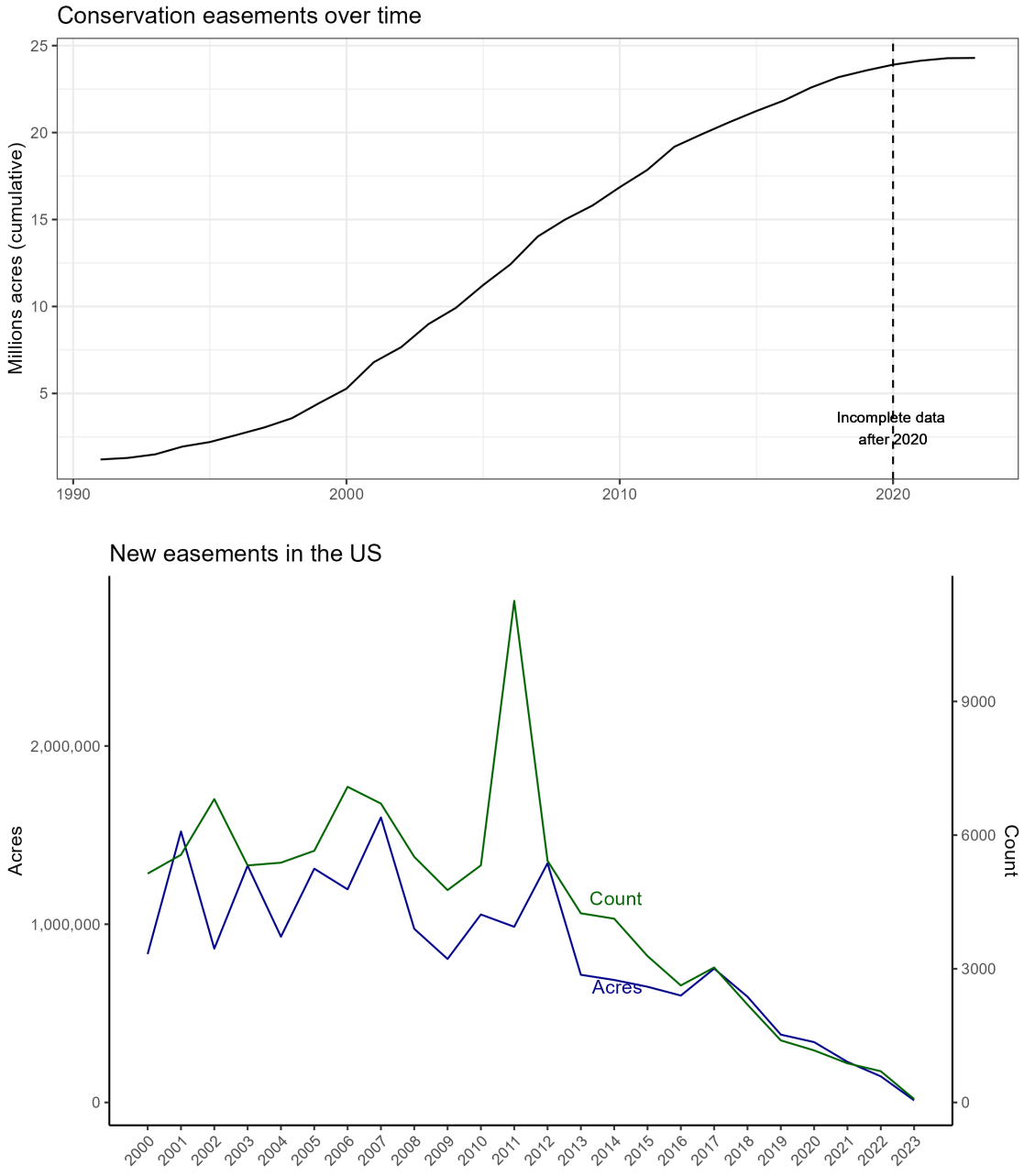
(a) Easement acreage by state over time



(b) Share of easements with missing establishment date

Notes: Panel (a) shows the cumulative growth of conservation easement acreage by state. Panel (b) shows the proportion of easement records lacking an establishment year, by state. Data from NCED, TNC, and NRCS. These figures are preliminary and will be updated with the latest data additions.

Figure 16: Conservation Easement National Trends [PRELIMINARY — TO BE UPDATED WITH LATEST NRCS/TNC/STATE ADDITIONS]



Notes: Figures show national trends in conservation easement establishment. These figures are preliminary and will be updated with the latest data additions.

Figure 17: Effect of easement proximity on interconnection, by distance [TODO: rerun with latest specification]

[PLACEHOLDER: Updated coefficient plots showing easement effect at varying distance thresholds for wind and solar]

Figure 18: Effect of easements on interconnection, by land value [TODO: rerun with latest specification]

[PLACEHOLDER: Updated coefficient plots showing easement effect across land value distribution for wind and solar]

A.7 Additional Tables

Table 8: IRS: All Individual Returns With Noncash Charitable Contributions Reported on Form 8283, Easements

Year	**No. returns**	**No. donations**	**Schedule A** Total, $ billion	**Schedule A** Per return, $	**Share** % all donations
2015	3,766	4,767	2.3	599,974	3.7
2016	3,540	4,518	4.2	1,195,539	5.7
2017	4,823	6,502	3.6	746,364	4.3
2018	9,844	14,095	6.5	660,666	9.2
2019	6,005	8,025	8.4	1,405,165	11.6
2020	4,151	4,884	5.1	1,226,653	6.2
2021	4,320	5,354	7.0	1,616,787	6.0

Source: IRS Statistics of Income (SOI)